JOURNAL OF AIRCRAFT
Vol. 47, No. 2, March–April 2010

Aircraft Decompression with Installed Cockpit Security Door

Nihad E. Daidzic* and Matthew P. Simones†
Minnesota State University, Mankato, Minnesota 56001

DOI: 10.2514/1.41953

A zero-dimensional model of cockpit and cabin decompression with cockpit security door is presented. The hinged panels in the security door were modeled to account for the pressure-equalization dynamics in the case of cockpit decompression. A comprehensive isentropic and isothermal theoretical analysis is presented with many closed-form and asymptotic solutions. New analytical estimates for the total decompression time and the pressure half-time were derived. The simulations for typical corporate and large-transport-category airplanes with different cabin geometries, discharge coefficients, rupture cross-sectional areas, pressure altitudes, and cabin altitudes have been obtained. The case in which the cockpit depressurizes first and its effect on the cabin decompression and on the security door integrity has been extensively studied. The recently required cockpit doors may be hazardous for flight crew in the case cockpit depressurizes first and other venting and blowout panels malfunction or are too slow to respond. The resulting pressure differential between the cockpit and the cabin can create instantaneous forces in excess of 80 kN on the cockpit security door. In addition, this puts the crew in danger due to explosive decompression on the time scale of 100 ms and increases the possibility of the security door being blown out of the frame.

Nomenclature

F	=	force, N or lb (1 lb $\approx$ 4.45 N)
g	=	gravitational acceleration, m^2/s or ft^2/s
h	=	altitude, m or ft (1 m $\approx$ 3.28 ft)
m	=	mass of air, kg or lb
$\dot{m}$	=	mass flow rate, kg/s or lb/s
p	=	pressure, Pa or psi (1 psi $\approx$ 6894.7 Pa)
$\tilde{p}$	=	pressure ratio (p_c/p_a)
R	=	gas constant, J/kg K (287 J/kg K for dry-air mixture)
T	=	temperature (absolute), K
Θ	=	pressure decay half-time, s
θ	=	angle of the swing panel, rad
κ	=	isentropic (adiabatic) coefficient of expansion (1.4 for dry-air mixture)
ρ	=	air density, kg/m^3
τ	=	time constant, s
τ	=	decompression (total) time, s
τ	=	subcritical (subsonic) decompression time, s
Φ	=	pressure-ratio function
ψ	=	coefficient
ψ'	=	coefficient
Ω	=	supercritical (choked flow) decompression time, s

Subscripts

ACM	=	air cycle machine (air pack)
a	=	atmospheric (environmental)
c	=	chamber
cb	=	cabin
cc	=	cockpit
control	=	controlled leak (outflow valve)
i	=	inlet/in
leak	=	uncontrolled leak
o	=	outlet/out

Received 1 November 2008; accepted for publication 23 November 2009.

*Associate Professor of Aviation, Adjunct Associate Professor of Mechanical Engineering, Airline Transport Pilot, Federal Aviation Administration Certified Flight Instructor for Airplanes and Gliders, Aviation Department, Armstrong Hall 324E; Nihad.Daidzic@mnsu.edu. Member AIAA (Corresponding Author).

†Graduate Student, Mechanical Engineering. 205 Trafton Science Center. Student Member AIAA.

I. Introduction

AN UNPROTECTED human organism is not adaptable to the hazardous factors of very-high-altitude environment. Extended exposure to low atmospheric pressure and temperature could be fatal for unprotected human. The risk of death or irreversible serious illnesses/injuries increases exponentially with the decrease of atmospheric pressure. Therefore, the flight crew and the passengers must use protective systems to maintain near-sea-level (SL) local pressure and temperature. Passive protective systems such as pressurized cabins are an excellent choice, as they make human activity not much different from that at low altitudes. Existing modern civilian jet airplanes are flying at high altitudes, some of them exceeding 45,000 ft. French–British supersonic passenger jet Concorde regularly cruised at altitudes of 55,000–59,000 ft, where the environmental pressures and temperatures are extremely low. Physiologically, these Concorde altitudes can be regarded as space-equivalent zones. According to the International Civil Aviation Organization, the Federal Aviation Administration (FAA), and the Joint Aviation Authority, flights above 51,000 ft would require pressurized suits. The current aviation regulations also say that at no time could airplane cabin altitude (CA) exceed 40,000 ft, and it could not surpass 25,000 ft for more than 2 min.

For example, at 40,000 ft (12,200 m), the International Standard Atmosphere (ISA) pressure is only about 18.8 kPa (2.73 psi), and the air temperatures are about −56.5°C (217 K). The boiling temperature of water at this atmospheric pressure is about 59°C (332 K). Above 63,000 ft or 19,200 m (*Armstrong* line), the ISA environmental pressure drops below 6.3 kPa (0.91 psi) and the boiling temperature of water reaches the normal human body temperature (about 37°C). Any prolonged exposure to such an environment could lead to ebullism, anoxia, and ultimate death, after several minutes. These are indeed very hostile conditions for human life. A good overview of the effects of hypoxia, dysbarism, embolism, anoxia, ebullism, and other high-altitude aeromedical factors of the human organism can be found in a number of papers dealing with aviation and space medicine [1–11].

A thin, yet very strong, structure of the airplane pressure vessel provides a safety cocoon that protects pilots and passengers from the lethal environmental effects. However, accidents caused by slow, rapid, or explosive decompression have occasionally led to the loss of airplanes and/or human lives. Especially today, in the age of a renewed push toward the space tourism and suborbital passenger

commercial flights and more frequent low-Earth-orbit and deep-space manned flights, the problem of chamber decompressions deservedly regained our attention. In suborbital and orbital flights, the additional risks, such as the shower of the ultrafast micrometeorites, can occur [12,13]. Such micrometeorites can punch large holes in the aircraft/spacecraft structure, causing rapid decompressions. Considering the increased frequency and duration of the future suborbital and orbital tourism and scheduled commercial flights, the decompression problems and associated hazards have to be addressed again. In addition, the installation of the new reinforced flight-deck security door that seals the cockpit from the cabin during the flight introduced some, perhaps unexpected, risks.

A simplified altitude profile of a typical high-altitude commercial aircraft flight is shown in Fig. 1. Title 14 of the Code of Federal Regulations (CFRs), commonly known as Federal Aviation Regulations, restricts maximum CA to 8000 ft (CFR Sec. 25.841 [14]). At 10,000 ft the CA cockpit warning is issued, and at a CA of 14,000 ft, the passenger oxygen mask will deploy. Typically, in commercial operations, the cabin rates of climb are set to no more than 500 fpm, and rates of descent are not more than 300 fpm to prevent any passenger discomfort. In most airplanes, the modern pressurization/environmental system is completely automated, requiring minimum input from the crew.

In the early jet age, the rapid-decompression accidents and the subsequent loss of human lives were relatively frequent [15–17]. Several British-made *Comet* civilian jets (historically, the first passenger jets in commercial service) were lost due to the structural failures and rapid/explosive decompressions. In the early 1950s, the problem of material fatigue was not well understood. Accordingly, serious consideration has been given to the topic of cabin decompression during the same period, partly also due to the development of human space programs in the United States and the former U.S.S.R. and the growth of the high-altitude passenger jet traffic. Occasionally, incorrect maintenance of the airframe [15,16], instruments, equipment, inappropriate operations [18], and engine blade separation [17,19] led to in-flight failures and accidents that sometimes resulted in a high human toll [16,17].

The recent FAA-mandated installation of reinforced cockpit (flight-deck) security (safety) doors (Title 14 CFR Sec. 25.795 [20], Sec. 121.313 [21], and Sec. 129.28 [22]), intended to prevent unauthorized intrusion into the cockpit during flight, presents a new, perhaps unforeseen, danger. In the case of rapid cockpit decompression, an extreme force can be exerted on the security door. Such a scenario can occur due to hail damage of the cockpit windshield, bird strike, engine blade separation, crack propagation, meteorite strikes at very high altitudes, etc. In the case of a pressure differential of 41 kPa (6 psi) between the cockpit and the cabin, with a door surface area of 2 m^2 (21.5 ft^2), about 82 kN (18,500 lb) of force can be instantaneously exerted on the door and its frame. The pressure differential and the force on the sealed cockpit door might be too much for the frame structure to handle if the cockpit depressurizes first. Passive and active internal venting (dado panels) may malfunction, get clogged by flying debris, or simply not react fast enough to relive the pressure differential on the security door.

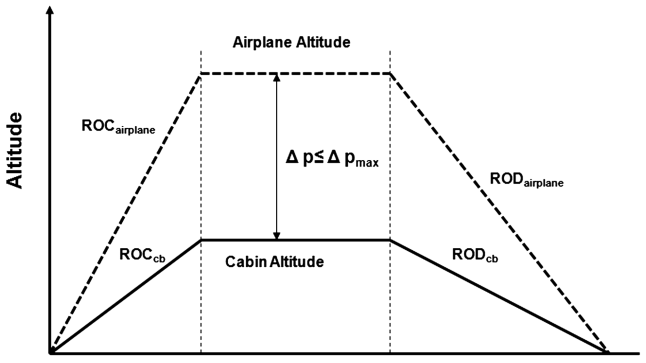

Fig. 1 Simplified altitude flight profile and airplane and cabin *cb* pressure changes for a typical commercial flight (not to scale).

A loose, heavy, armored door can be much more dangerous than no door at all (or light door), as it could seriously injure or kill the flight crew, jam and/or destroy flight controls, damage and destroy flight instruments, and create mayhem in the cockpit. Such a scenario is incredibly dangerous, as it may prevent emergency descent. The rise of pressure differential and the force across the cockpit security door may well be much quicker than the designed venting system is capable of handling.

Passive and active venting between various pressurized chambers, swing panels, and blowout panels in the security door are supposed to minimize these risks [23–25]. But it is not clear that the existing airplanes in service, now retrofitted with the intrusion-proof flight-deck doors, have enough fast bypass-venting capacity to timely reduce the peak forces on the door. This paper is also a contribution toward better understanding of the complex aircraft decompression phenomena and interaction with the security door pressure-equalization panels.

A search of the National Transportation Safety Board (NTSB) data on decompression accidents and incidents yielded only eight decompression events in the past four years in the United States. Out of these, only one was a fatal accident. This definitely speaks well for the safety of the pressurized cabin in flight, but it is not the whole picture by any means. According to 49 CFR Part 830 [26], the NTSB needs to be notified only under certain circumstances. There is no direct requirement to notify the NTSB when an aircraft has experienced decompression. However, according to other statistics, the decompression incidents are much more frequent and many are never reported [17,27].

Another source of information concerning events of decompression comes from a voluntary reporting program in the United States called the Aviation Safety Reporting System (ASRS). This is a site set up by NASA and the FAA that encourages those involved with aviation to report events, such as accidental oversights, whose occurrence would encourage future policy development, human factors research, education, and training. The results of a study of the events in the ASRS and Australian Transportation Safety Board databases are listed in [27]. The authors found that 32% of the reported causes were due to the pressurization controller. The next most common cause was the pressurization source. The remaining 21% were reported as structural failures. The authors of the report also suggest that actually 40–50 rapid decompressions per annum occur worldwide, but many stay unreported as long as there is no damage, serious incapacitation, or injuries involved.

One of the most infamous accidents involving structural failures of airframes and cabin decompression occurred in 1988 on an Aloha Airline's Boeing 737-297 (N73711) near Maui, Hawaii [16]. According to the NTSB report, Flight 243 was at flight level (FL) 240 when a section of the upper fuselage separated from the aircraft near the front passenger section. Approximately 18 ft were torn off. Although the flight did make a successful landing in Maui, one flight attendant was swept overboard from the force of the explosive decompression and many passengers were injured from flying debris. In-flight decompression incidents and accidents are thus relatively common even today [18,19,28–30].

Haber and Clamann (H-C) [31] delivered a report in 1953 that was considered a general theory of aircraft cabin decompressions. Their model was zero-dimensional, assuming uniform pressure, temperature, and density in the chamber. In addition to developing theoretical polytropic models of decompression, the authors also performed measurements using small chambers. Their experiments resulted in an average polytropic exponent of $n = 1.16$ averaged over *75* decompression experiments. H-C also provided analytical expression for the decompression time (DT), which includes critical and subcritical outflow, but which also requires a separate diagram to be used in calculating their pressure-ratio function. Still today, H-C theory is considered a standard in aircraft decompression analysis. The first published paper on cabin decompression comes from Demetriades [32]. The author examines isentropic decompression of a pressurized cabin in vacuum (spacecraft). Demetriades estimated relationships between the initial and final pressures as a function of DT. No repressurization was considered and the outflow did not

include discharge coefficient correction. The idea in his paper was to examine decompression dynamics and develop countermeasures that would secure early human space flights. Mavriplis [33] published an extensive lumped-parameter study of the decompression of pressurized cabins for both atmospheric vehicles (airplanes) and spacecraft. Many closed-form solutions for isothermal, polytropic, and isentropic decompressions were derived. Mavriplis also studied the effect of repressurization for aircraft and spacecraft. In the case of three communicating compartments, the Runge–Kutta fourth-order numerical simulation was used to solve the complex interconnected-chambers decompression dynamics. Mavriplis, just as with previous authors, did not consider the dynamics of the valves and panels that separate those compartments. However, we found the Mavriplis work to be the most useful for our own investigations. Langley [23] studied compartmentalization of aircraft using the marine ship experience and suggested using it in airplane design. By sealing off different compartments, decompression can be prevented from propagating throughout the whole airplane. That would, however, imply that some passengers could be sacrificed in a sealed-off compartment, which would not be an acceptable solution today. Jakovlenko [34] calculated the excess pressure in human lungs and the dangers of dysbarism in case of space cabin decompression. The main feature of his mathematical model was simultaneous computation of the air outflowing from human lungs and lung expansion due to cabin decompression, resulting in good agreement of experimental results and theoretical predictions. Schroll and Tibbals [35] have presented a zero-dimensional model and associated computer program with a graphical user interface that simulates rapid aircraft cabin decompression. Their model is based on a simple isentropic outflow and cabin air state change to obtain depressurization dynamics. They used discharge coefficient of 0.7 corresponding to rupture with sharp edges. The main objective of their work was to estimate the amount of emergency oxygen supply accounting for emergency descent toward safe breathable altitudes. However, no aircraft emergency descent performance, multiple compartments, venting system dynamics, and security door were included. The only paper dealing with the problems of cockpit security door that we could find was by Bréard et al. [36]. The authors used commercial 3-D computational fluid dynamics (CFD) code to calculate the external velocity and pressure distribution around the cockpit of a cruising airplane and the internal flight-deck pressure distribution caused by side-window failure. The CFD code solves the Navier–Stokes equations with turbulence quantities. Bréard et al. simulated window panel break-up in which a cockpit depressurizes very quickly, and then they calculated the force on the blowout panels, pressure differential, and the dynamics of cabin decompression. However, little insight has been given about their model limitations and capabilities. Recently, Pratt [25] considered the dynamics of passive and active venting blowout panels and hinged doors between different pressurized airplane compartments in case of rapid decompression. Mass and the moment of inertia of the panels were considered, but otherwise the model seems to be too simplistic. From the results it is very difficult to estimate the reliability of Pratt's model. Some inconsistencies, errors, and inaccuracies were noted in his work. No cockpit security door and hinged panels were modeled in Pratt's work.

II. Mathematical Model

A. General Formulation

A simple zero-dimensional (lumped-parameter) mathematical model with spatially uniform air pressure, temperature, and density temporal change in the airplane's pressurized vessel is presented. In general, the thermodynamic changes in the air are irreversible and polytropic [31,33,37], as they include heat transfer and water phase change, but in the case of explosive decompression (less than 500 ms) or rapid decompression (less than 10 s), a reversible adiabatic change can be assumed with reasonable accuracy. The case of slow decompression (more than 2 min) can be approximated by isothermal expansion, in which the air cooling due to expansion will be compensated by the aircraft's environmental system; in between (say, 10–120 s), the polytropic process must be used. This requires an additional energy, and possibly entropy, equation in a differential (or integral) form to be solved simultaneously.

In this study we did not separately model the pressurized cargo and avionics compartments. The passive and active venting systems enabling communication with the cabin are assumed to be instantaneous. Other assumptions and limitations adopted in the present model are as follows:

1) The effect of relative humidity (RH) and latent heat of condensation and sublimation is neglected. The airplane environmental air is usually very dry.

2) The cabin and the cockpit volume do not change with the air pressure. In reality, there is a very small volume change caused by pressurization, but it will be neglected here.

3) The atmosphere is regarded as an infinite volume of air and the atmospheric pressure does not change with the outflow of the cabin or cockpit air.

4) Airplane maintains altitude and the atmospheric pressure is constant. In reality, this means that no emergency descent maneuver is initiated.

5) Air is regarded as an ideal (perfect) gas.

6) The air properties are uniform throughout the volume. No spatial dependence is modeled. The model has lumped parameters.

7) The diabatic mass flow rate through the rupture is accounted for by using the experimental discharge coefficient.

8) There is no cockpit air RAM pressure recovery if the side window breaks.

9) The local outside pressure variations along the fuselage caused by variable local velocities are accounted for by using an equivalent average flight level (altitude).

10) The dynamics of passive and active venting through the pressurized cargo departments or other passages and chambers were neglected in this study. It is assumed that the cargo air is immediately available for cabin decompressions.

We are modeling processes in the cockpit and cabin-cargo compartments separately. In this study, the only possible communication between the cockpit and cabin is through the hinged flap/panel in the cockpit security door, with the purpose of relieving the excessive pressure differential when flight-deck decompression occurs first. This communication is one way only, i.e., the pressure cannot be equalized through the door panels if the cabin depressurizes first. In general, decompression can occur in the passenger cabin, crew cockpit, or both in the same time.

Furthermore, we assume the decompression to occur during level cruise flight. The airplane emergency descent was not modeled here. It normally would take a minimum of 6–10 s for pilots to initiate the emergency descent: donning the oxygen masks, establishing oxygen flow and communication, checking bleed air and air packs, and perhaps reconfiguring the airplane before the descent is started. In addition, the atmosphere is quite flat ($\mathrm{d}p/\mathrm{d}h$ is small) at cruising jet altitudes, and no significant change in atmospheric pressure occurs for an altitude change of several thousand feet. Normally, it would take a well-trained and coordinated crew over 1 min to descend below 25,000 ft from the most common cruising altitudes (33,000–39,000 ft).

In Fig. 2, the simplified schematic drawing of the cockpit-cabin pressure vessel is shown. It is assumed in this study that cabin(s) can communicate with cargo compartment(s) instantaneously and without any resistance, making cargo air available in decompression. ISA conditions will be used when calculating environmental air variables. The airplane's environmental pressurization and air-conditioning system (air packs) are continuously providing relatively dry (RH of 30–35%) conditioned air to the cabin and cockpit [24,38,39]. Because of the installed security doors, which are closed and locked during the flight, these two air reservoirs do not communicate. Conditioned air is continually supplied to the cabin and cockpit ($\dot{m}_i$) by separate air packs, to maintain pressure and offset ever-present uncontrolled vessel leakage. Outflow valve(s) operate to maintain the cabin pressure in a specified range [24]. The safety relief valve will open if necessary to reduce the excess pressure differential, thus protecting the structural integrity of the pressure vessel. The

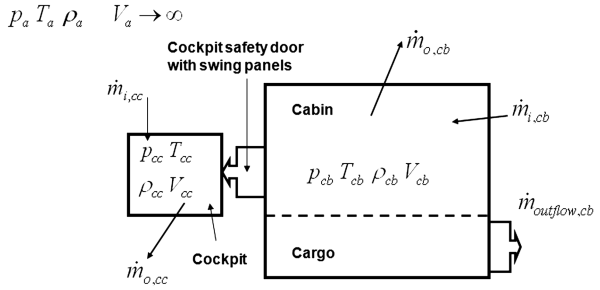

Fig. 2 Simplified schematic of the airplane pressurization. Passenger cabin and cargo compartment communicate without any delay. No other passive or active venting dynamics between these chambers were modeled (not to scale).

airplane's pneumatic bleed-air pressurization and environmental control systems (ECSs) for large transport-category airplanes, for example, are described in [24] and, particularly for the Boeing 767-300ER, in [38,39].

In a level cruising flight at constant airspeed, the inflow of the air-conditioned air from the air packs is assumed to be constant. The mixture of fresh and filtered recirculated air will offset air lost due to uncontrolled leakage, and the excess air will leave the pressure vessel through the outflow valve as controlled discharge. Normally, air is exchanged many times per hour in an airplane cabin. Hunt et al. [38,39] examined cabin environment, air quality, and pressurization for a Boeing 767-300ER, a popular twin-engine wide-body commercial jet transport.

The integral mass balance for the pressurized chamber, when the outflow valve is not fully closed, can be written as

$$\frac{\mathrm{d}m_c}{\mathrm{d}t} = \dot{m}_{\mathrm{ACM}} - \dot{m}_{\mathrm{leak}} - \dot{m}_{\mathrm{control}} = 0 \qquad \dot{m}_{\mathrm{ACM}} = \mathrm{const} \tag{1}$$

We also assumed the inflow of air-conditioned pressurized air $\dot{m}_{\mathrm{ACM}}$ to be steady for the constant engine fan (N_1) speed. When the outflow valve is fully closed, $\dot{m}_{\mathrm{control}} = 0$. Accordingly, the outflow valve(s) cannot compensate for any additional uncontrolled leaks, $\dot{m}_{\mathrm{ACM}} - \dot{m}_{\mathrm{leak}} = 0$, where $\dot{m}_{\mathrm{ACM}} = \mathrm{const}$.

The maximum pressure differential is a structural limit that restricts the airplane's maximum certified flight altitude, so that CA does not exceed 8000 ft (10. 92 psi or 75.2 kPa ISA). For example, a Boeing 767-300ER has maximum pressure differential of 8.6 psi, restricting the airplane's maximum certified altitude to 2.32 psi (43,100 ft), although the B767's aerodynamic ceiling is higher. Recently, there has been a renewed interest to lower the maximum CA to 6000 ft, which would require higher pressure differentials or flying at lower altitudes. It is very unlikely that airplanes will fly at lower altitudes, so the airplane manufacturers will have to build even stronger pressure vessels, perhaps by using advanced lightweight composite materials (e.g., new Boeing 787 or Airbus 350).

Conditions inside the cabin are defined as p_{cb}, T_{cb}, and ρ_{cb}. Similarly, for the cockpit, we have p_{cc}, T_{cc}, and ρ_{cc}. Outside (atmospheric) conditions are defined as p_a, T_a, and ρ_a. Atmosphere is regarded as a perfect infinite sink. When rupture occurs in the fuselage structure, the pressure differential will cause outflow of pressurized chamber air until the internal pressure stabilizes with respect to the existing inflow of the conditioned air and the outflow caused by the lower local atmospheric pressure.

The temporal change of the chamber (cabin or cockpit) air pressure can be estimated from an integral mass balance equation. We use the subscript c to denote any pressurized airplane chamber, and in our case, it can be either cabin or cockpit-cargo combination:

$$\frac{\mathrm{d}m_c}{\mathrm{d}t} = \dot{m}_i - \dot{m}_o \tag{2}$$

where $\dot{m}_o$ is uncontrolled outflow through the rupture in the pressure vessel and $\dot{m}_i$ is the repressurization inflow of air, which is in excess of the air required $\dot{m}_{\mathrm{ACM}}$ to offset the regular uncontrolled leaks in the structure. In this way, we can simulate repressurization scenarios in which extra air is pumped into the cabin for the purpose of reducing the rate of pressure drop and increase of the CA. However, repressurization (recompression) is technically difficult to achieve and has been considered for many years. In existing commercial airplane designs, it is not possible to achieve significant repressurization, and so $\dot{m}_i$ will always be zero in our simulations. However, we will carry on derivations with repressurization in mind, as that will provide generality to our approach and can be helpful for future studies on recompression rates required in various decompression situations.

In the case of decompression, the outflow valve would close quickly, unsuccessfully trying to maintain the chamber pressure. Therefore, we are primarily interested in the cases in which the outflow valve(s) are already fully closed. If the outflow valve(s) were able to compensate for the additional leaks by closing some more, that would have been a trivial case, not requiring our analysis. Since the chamber volume does not change, and by using the ideal-gas law, the total change of cabin air density is

$$\frac{1}{RT_c}\cdot\frac{\mathrm{d}p_c}{\mathrm{d}t} - \frac{p_c}{RT_c^2}\cdot\frac{\mathrm{d}T_c}{\mathrm{d}t} = \frac{1}{V_c}(\dot{m}_i - \dot{m}_o)$$
$$\Rightarrow \frac{\mathrm{d}p_c}{\mathrm{d}t} = \frac{nRT_c}{V_c}(\dot{m}_i - \dot{m}_o) \tag{3}$$

where n is the unknown polytropic coefficient of expansion. Obviously, to solve for the three unknowns of chamber air pressure p_c, absolute temperature T_c, and air density ρ_c, one needs three simultaneous equations; differential and/or algebraic. The above derived mass balance provides one equation, and the ideal-gas law with particular relationships between thermodynamic variables (equation of state) provides the second equation. However, we do need a third equation, and the energy equation is the best candidate for that.

The uncontrolled outflow from the pressurized chamber to outside environment will occur either under sonic (choked or critical/supercritical) or subsonic (subcritical) flow conditions in the throat of the rupture [32,33,37,40–43]. For sonic conditions to occur, a certain critical ratio between the chamber and the environmental air pressure must exist.

If the chamber air pressure is roughly twice, or more, the environmental air pressure ($p_c^* = 1.893 p_a$) and the mass flow rate through the rupture will be at theoretical maximum, with the local Mach number in the rupture throat equal to one. Otherwise, the flow will be subcritical. Accordingly, our mathematical model will be separated into two parts, one modeling choked flow and the other modeling subsonic flow:

$$p_c \geq p_c^* \to \text{choked or sonic flow}\,(M = 1) \qquad \dot{m}_o = f(p_c)$$
$$p_c < p_c^* \to \text{subsonic flow}\,(M < 1), \qquad \dot{m}_o = f(p_c, p_a)$$

When the Mach number reaches 1 in the narrowest part of the opening (throat) of the simple rupture, the mass flow rate is at the theoretical maximum. Then the outflow depends on the upstream (chamber) pressure only, but not at all on the downstream pressure [32,33,37]:

$$\dot{m}_{o,\max} = C_D A \psi \frac{p_c}{RT_c}\sqrt{\kappa RT_c} = \frac{A_{\mathrm{eff}}\psi\sqrt{\kappa}}{\sqrt{RT_c}}p_c = A_{\mathrm{eff}}\psi'\frac{p_c}{\sqrt{RT_c}} \tag{4}$$

Here, $C_D < 1$ is the discharge coefficient and A is the cross-sectional area of the rupture (opening, crack, hole, compromise, puncture). The discharge coefficient is the ratio between the actual diabatic (or possibly fast adiabatic) irreversible outflow and the theoretically maximum possible or isentropic outflow [37]. The product of the rupture cross-sectional area and the discharge coefficient is actually the effective cross-sectional outflow area A_{eff}. For a dry-air mixture, we have $\kappa \equiv c_p/c_v = 1.4$, $R = 287$ J/kg K, and

$$\psi \equiv \left(\frac{2}{\kappa+1}\right)^{\frac{\kappa+1}{2(\kappa-1)}} = 0.5787 \qquad \psi' \equiv \psi\cdot\sqrt{\kappa} = 0.6847$$

when the chamber air versus atmospheric pressure ratio (PR) decreases to a critical ratio:

$$\frac{p_a}{p_c^*} = \left(\frac{2}{\kappa+1}\right)^{\frac{\kappa}{\kappa-1}} = 0.5283 \Rightarrow p_c^* = 1.893 \cdot p_a \tag{5}$$

The outflow transitions smoothly from choked to subsonic (subcritical) and the mass flow rate now depends on the outside (atmospheric) pressure as well [32,33,37,40–43]:

$$\dot{m}_o = C_D A \bar{u} \rho_c = A_{\text{eff}} \sqrt{\frac{2\cdot\kappa}{\kappa-1}\rho_c p_c \left[\left(\frac{p_a}{p_c}\right)^{\left(\frac{2}{\kappa}\right)} - \left(\frac{p_a}{p_c}\right)^{\left(\frac{\kappa+1}{\kappa}\right)}\right]}$$
$$= A_{\text{eff}} p_a \left(\frac{2\cdot\kappa}{\kappa-1}\right)^{1/2} \left(\frac{1}{RT_c}\right)^{1/2} \tilde{p}^{\frac{\kappa-1}{\kappa}} [1 - \tilde{p}^{\frac{1-\kappa}{\kappa}}]^{1/2} \tag{6}$$

where $\tilde{p} = p_c/p_a$, is the dimensionless chamber-to-environment pressure ratio, with the cross-sectional averaged outflow velocity

$$\bar{u} = \sqrt{\frac{2\cdot\kappa}{\kappa-1} RT_c \left[1 - \left(\frac{1}{\tilde{p}}\right)^{\frac{\kappa-1}{\kappa}}\right]}$$
$$= \left(\frac{2\cdot\kappa}{\kappa-1}\right)^{1/2} (RT_c)^{1/2} \left[1 - \left(\frac{1}{\tilde{p}}\right)^{\frac{\kappa-1}{\kappa}}\right]^{1/2} \tag{7}$$

Although the air pressure change in the chamber can be isothermal, isentropic, or, in general, polytropic, the discharge process through the rupture is modeled as isentropic. This is a reasonable assumption, as the outflow is very rapid and the puncture nozzle is relatively short. However, to account for the friction, jet contraction, and diabatic outflow, a discharge coefficient C_D is used [31,37,40–43]. The easiest way to estimate the discharge coefficient is to measure it, but this is of no practical use, as the exact geometry of the rupture is unpredictable in most cases and can vary dramatically. Using the complicated, expensive, and time-consuming CFD codes just to model the discharge coefficient takes us away from the fundamental problem and does not increase the accuracy significantly. The best way to deal with this uncertainty in discharge coefficient is to perform sensitivity analysis by varying the value of C_D.

In Fig. 3, the dynamics are shown of the chamber's decompression into atmosphere or vacuum, with and without repressurization. If the atmospheric pressure has nonzero value, then the transition to subcritical flow will occur at a chamber pressure roughly equal to 1.9 times the atmospheric pressure. In addition, the minimum pressure to which the chamber pressure can decrease is the atmospheric pressure p_a. In the case of practical vacuum (spacecraft), the pressure will decrease to zero and the recompression from reserve air will keep the chamber pressure higher than vacuum.

B. Isothermal Model of Chamber Decompression

The simplest possible form of the energy balance equation is to assume that the uniform chamber temperature stays constant ($T = \text{const.}$) during decompression, resulting in isothermal change, where $n = 1$ in Eq. (3):

$$\frac{\mathrm{d}p_c}{\mathrm{d}t} = \frac{RT_c^o}{V_c}(\dot{m}_i - \dot{m}_o)T_c = T_c^o \tag{8}$$

The constant chamber temperature approximation during slow decompression results in

$$\dot{m}_o = \dot{m}_{o,\max} = K \cdot p_c$$
$$K = \frac{C_D \cdot A \cdot \psi \cdot \sqrt{\kappa}}{\sqrt{R \cdot T_c^o}} = \frac{A_{\text{eff}} \cdot \psi'}{\sqrt{R \cdot T_c^o}} = \text{const} \tag{9}$$

It follows that the parameter K is directly proportional to the effective rupture area and inversely proportional to the square root of the initial (constant) air chamber temperature. Since the repressurization or recompression inflow is assumed to be constant, the differential equation is linear with constant coefficients and can be easily solved analytically:

$$\frac{\mathrm{d}p_c}{\mathrm{d}t} = \frac{RT_c^o \dot{m}_i}{V_c} - \frac{RT_c^o K}{V_c} \cdot p_c = A - B \cdot p_c \Rightarrow \frac{\mathrm{d}p_c}{\mathrm{d}t} + B \cdot p_c = A \tag{10}$$

As long as the outflow is choked, the chamber does not know or care about the outside environmental pressure. Decompression into vacuum (neglecting noncontinuum effects) will continue until equilibrium zero pressure is achieved, in which case Eq. (10) is valid and has the solution consisting of a particular and a homogeneous part:

$$p_c(t) = p_c^\infty \cdot (1 - e^{-Bt}) + p_c^o \cdot e^{-Bt} \qquad p_c^\infty = \frac{A}{B} \qquad \tau = \frac{1}{B} \tag{11}$$

The reciprocal value of constant B is actually the time-constant τ of the outflow process and

$$\xi = \frac{RT_c^o}{V_c} \qquad A = \frac{RT_c^o \dot{m}_i}{V_c} = \xi \cdot \dot{m}_i$$
$$B = \xi \cdot K = \left(\frac{A_{\text{eff}}}{V_c}\right) \cdot \psi' \cdot \sqrt{R \cdot T_c^o} \tag{12}$$

The process of pressure change in Eq. (11) is a rather interesting one. We have two exponential functions, one decreasing monotonically with time from the initial chamber pressure to zero as described by the homogeneous solution and the other rising from zero and asymptotically approaching the final chamber pressure described by the particular solution and depending on the extra inflow of repressurization air. This analysis is strictly valid for isothermal spacecraft or suborbital aircraft decompression in practical vacuum.

The effect of repressurization is not only to maintain higher pressure than environmental, but also to reduce the rate of pressure drop, which is important for human physiological response and enables more time for countermeasures. The pressure drop now becomes

$$\frac{\mathrm{d}p_c(t)}{\mathrm{d}t} = -p_c^o \cdot B \cdot e^{-Bt} + A \cdot e^{-Bt} \tag{13}$$

from which it is obvious how repressurization reduces decompression rate. At the initial instant, the total pressure change rate is

$$\frac{\mathrm{d}p_c(0)}{\mathrm{d}t} = -p_c^o \cdot B + A \le 0 \tag{14}$$

The speed of pressure decrease in excess of 650 psi/s (4.48 MPa/s) may cause serious lung hemorrhage [33]. Although not a particular problem in an airplane cabin, unless total cabin destruction occurs almost instantaneously, it could be a problem in a cockpit.

Obviously, the choked outflow cannot continue for the entire time unless the outflow is in vacuum, and then only in an approximation. Demetriades [32] did not make this distinction in his study of depressurization of spacecraft cabins, but, in all honesty, it would not make a big difference, since pressures at which continuum vanishes

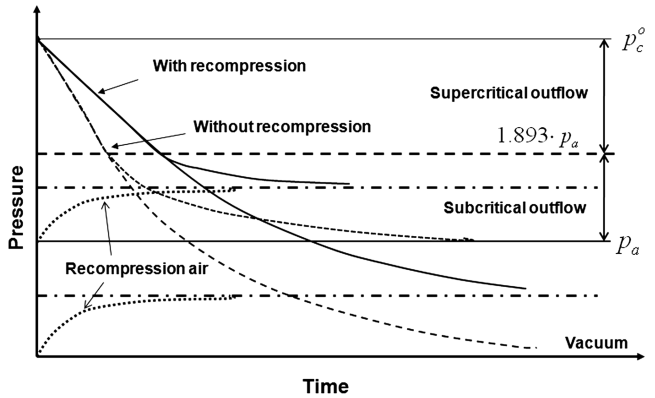

Fig. 3 Decompression processes into vacuum or finite atmosphere with and without repressurization (recompression) (not to scale).

are much below the minimum pressure required for human survival. The final chamber pressure reached in vacuum is thus

$$\lim_{t\to\infty} p_c(t) = p_c(\infty) = p_c^{\infty} = \frac{A}{B} = \frac{\dot{m}_i}{K} = \frac{\dot{m}_i}{A_{\text{eff}} \cdot \psi'} \sqrt{R \cdot T_c^o}$$

The larger this ratio, the slower the chamber will decompress and the higher the final pressure will be. This method is used in spacecraft decompression prevention.

In the case when repressurization is negligible, the critical outflow into vacuum will only contain the homogeneous solution of the differential equation (11). However, when discharged into atmosphere, the choked outflow will continue only as long as the PR is higher than critical:

$$p_c(\Omega) = p_c^o \cdot e^{-B\cdot\Omega} = 1.893 \cdot p_a$$

The elapsed time for which the choked chamber isothermal expansion exists can be now estimated from

$$\Omega = \tau \cdot \ell_n(0.5283\tilde{p}^o) = \left(\frac{V_c}{A_{\text{eff}}}\right) \frac{\ell_n(0.5283\tilde{p}^o)}{\psi' \sqrt{RT_c^o}} \tag{15}$$

where $\tilde{p}^o = p_c^o/p_a = \text{const}$ is the initial chamber-to-environment pressure ratio. This is the same result obtained previously in [33]. In the case of chamber air temperature of 296 K, this reduces to a simple expression when $\tilde{p}^o \geq 1.893$:

$$\Omega \approx \frac{1}{200}\left(\frac{V_c}{A_{\text{eff}}}\right) \ell_n(0.5283\tilde{p}^o) \qquad \tau \approx \frac{1}{200}\left(\frac{V_c}{A_{\text{eff}}}\right) = B^{-1} \tag{16}$$

If the recompression air is pumped into the chamber, the supercritical (choked) DT is calculated from Eq. (10):

$$\int_{p_c^o}^{1.893 p_a} \frac{\mathrm{d}p_c}{A - B \cdot p_c} = \int_0^{\Omega} \mathrm{d}t = \Omega$$

$$\Rightarrow \Omega = \frac{1}{200} \cdot \left(\frac{V_c}{A_{\text{eff}}}\right) \cdot \ell_n\left(\frac{A - B \cdot p_c^o}{A - 1.893 \cdot p_a \cdot B}\right) \tag{17}$$

Even small recompression can significantly reduce the pressure drop rate and lower the final CA. In retrospect, isothermal approximation is inaccurate for rapid decompression, as it would be impossible to maintain constant air temperature in rapid expansions.

A nonlinear ordinary differential equation (ODE) for the isothermal change with subsonic outflow in the rupture throat and with constant repressurization rate can be written as

$$\frac{\mathrm{d}\tilde{p}}{\mathrm{d}t} = \frac{RT_c^o}{p_a V_c} \cdot \dot{m}_i - \frac{A_{\text{eff}}}{V_c} (R \cdot T_c^o)^{1/2} \left(\frac{2\cdot\kappa}{\kappa - 1}\right)^{1/2} \tilde{p}^{\frac{\kappa-1}{\kappa}} (1 - \tilde{p}^{\frac{\kappa-1}{\kappa}})^{1/2} \tag{18}$$

In the case of the initially constant chamber air temperature of 296 K and no repressurization, this reduces to

$$\frac{\mathrm{d}\tilde{p}}{\mathrm{d}t} \approx -771 \cdot \frac{A_{\text{eff}}}{V_c} \cdot \tilde{p}^{\frac{2}{7}} \cdot (1 - \tilde{p}^{\frac{-2}{7}})^{1/2} \tag{19}$$

The following indefinite integral represents the isothermal subsonic PR function and can be represented in terms of elementary functions:

$$\Phi_t(\tilde{p}) = \int_1^{\tilde{p}} \frac{\mathrm{d}\tilde{p}}{\tilde{p}^{\frac{2}{7}} \cdot (1 - \tilde{p}^{\frac{-2}{7}})^{1/2}} = \int_1^{\tilde{p}} \frac{\mathrm{d}\tilde{p}}{\tilde{p}^{\frac{1}{7}} \cdot (\tilde{p}^{\frac{2}{7}} - 1)^{1/2}} = (\sqrt{\tilde{p}^{\frac{2}{7}} - 1})$$

$$\cdot \left(\frac{7}{5} \cdot \tilde{p}^{\frac{4}{7}} + \frac{28}{15} \cdot \tilde{p}^{\frac{2}{7}} + \frac{56}{15}\right) \tag{20}$$

The total subcritical isothermal decompression takes place between pressure ratios $\tilde{p}^o$ of 1.893 to 1. The DT for entire isothermal subcritical (subsonic) expansion without repressurization is now

$$\tau = \int_0^{\tau} \mathrm{d}t = \frac{\Phi_t(1.893)}{771}\left(\frac{V_c}{A_{\text{eff}}}\right) \approx 4.63 \cdot 10^{-3}\left(\frac{V_c}{A_{\text{eff}}}\right) \tag{21}$$

In the case when isothermal decompression starts in the subcritical range (entirely only subsonic outflow) with the same air temperature of 296 K, the DT becomes

$$\tau = 1.3 \cdot 10^{-3} \cdot \Phi_t(\tilde{p}^o) \cdot \left(\frac{V_c}{A_{\text{eff}}}\right) \qquad 1 \leq \tilde{p}^o < 1.893$$

$$\Phi_t(1) = 0 \tag{22}$$

The total isothermal DT is a sum of the supercritical and subcritical decompression times. For air at 296 K and no recompression, we obtain

$$\tau \approx 4.63 \cdot 10^{-3}\left(\frac{V_c}{A_{\text{eff}}}\right) \cdot [1 + 1.08 \cdot \ell_n(0.5283\tilde{p}^o)] \qquad \tilde{p}^o \geq 1.893 \tag{23}$$

The theoretical model of isothermal decompression derived here serves us sufficiently well in analyzing slow-decompression scenarios on the order of several minutes.

C. Isentropic Model of Chamber Decompression

The previous model assumed the isothermal chamber's change, which is a good approximation during slow decompressions (greater than 2–3 min). The model will now be expanded to include changes in both pressure and temperature during the isentropic (explosive or rapid) decompression. Such an isentropic (adiabatic and reversible or constant entropy) model in which heat transfer and irreversible effects have been neglected is more representative of rapid/explosive decompressions.

Using the first law of thermodynamics [37] for an isentropic process and employing the pressure–density–temperature relationship in the form of an ideal-gas law, one obtains familiar isentropic relationships:

$$\frac{T_c}{T_c^0} = \left(\frac{p_c}{p_c^0}\right)^{\frac{\kappa-1}{\kappa}} \Rightarrow T_c(t) = T_c^0 \cdot \left[\frac{p_c(t)}{p_c^0}\right]^{\frac{\kappa-1}{\kappa}} \tag{24}$$

This expression can be substituted into the mass balance equation (3) to obtain the expression in terms of the pressure rate:

$$\frac{1}{RT_c} \cdot \frac{\mathrm{d}p_c}{\mathrm{d}t} - \frac{p_c}{RT_c^2} \cdot \left(\frac{R \cdot T_c}{p_c \cdot c_p} \cdot \frac{\mathrm{d}p_c}{\mathrm{d}t}\right) = \frac{1}{V_c}(\dot{m}_i - \dot{m}_o) \tag{25}$$

Noting that the chamber pressure and temperature are now both functions of time, this equation can be reduced further using Eq. (4) for choked (supercritical) outflow, $n = \kappa$:

$$\frac{\mathrm{d}p_c(t)}{\mathrm{d}t} = \frac{\kappa R T_c}{V_c}(\dot{m}_i - \dot{m}_o) = (\kappa R)\left(\frac{\dot{m}_i}{V_c}\right) T_c(t)$$

$$- \left(\frac{A_{\text{eff}}}{V_c}\right)(\psi'\kappa\sqrt{R})\sqrt{T_c(t)}\, p_c(t) \tag{26}$$

However, temperature can be removed from Eq. (25) by using the isentropic relationships, resulting in

$$\frac{\mathrm{d}p_c(t)}{\mathrm{d}t} = (\kappa R)\varsigma\left(\frac{\dot{m}_i}{V_c}\right) p_c^{(\kappa-1)/\kappa} - \left(\frac{A_{\text{eff}}}{V_c}\right)(\psi'\kappa\sqrt{R})\varsigma^{1/2} p_c^{(3\kappa-1)/2\kappa} \tag{27}$$

where $\varsigma = T_c^0/(p_c^0)^{\frac{\kappa-1}{\kappa}}$ is a constant depending on the initial chamber conditions. There are no obstacles in numerically solving this equation. However, some approximate solutions can be deduced from Eq. (27).

In the case of polytropic change, one need only to replace the coefficient of adiabatic (isentropic) expansion κ with the polytropic coefficient n. The problem is that the polytropic coefficient is not known a priori and will depend on the rate of heat transfer and other irreversible effects. In the case of isothermal change without repressurization, $n = \kappa = 1$, Eq. (26) reduces to Eq. (10).

Let us now analyze the nonlinear ODE in Eq. (27) more closely. The first term on the right-hand side (RHS) is a term dependent on the repressurization (recompression) air and can be set to zero for all practical purposes in today's airplanes. The second term on the RHS is thus normally much larger than the first, resulting in

$$\frac{\mathrm{d}p_c(t)}{\mathrm{d}t} = -\left(\frac{A_{\mathrm{eff}}}{V_c}\right)(\psi'\kappa\sqrt{R})\varsigma^{1/2}p_c^{(3\kappa-1)/2\kappa} \tag{28}$$

This ODE can be separated and integrated analytically to yield

$$p_c(t) = p_c^0\left[1 - \left(\frac{A_{\mathrm{eff}}}{V_c}\right)\left(\psi'\frac{1-\kappa}{2}\sqrt{RT_c^0}\right)t\right]^{2\kappa/(1-\kappa)} \tag{29}$$

This is the same solution obtained originally by Demetriades [32], which was derived here independently using a slightly different approach. Particularly for air at the initial cabin temperature of 296 K (23°C),

$$\left(\frac{p_c}{p_c^0}\right)^{\frac{-1}{7}} \approx 1 + 40\left(\frac{A_{\mathrm{eff}}}{V_c}\right)\cdot t \tag{30}$$

This expression is similar to the expression obtained in [32] for the depressurization of sealed spacecraft cabins. The duration of the choked (supercritical) decompression is thus

$$\Omega \approx 0.025\left(\frac{V_c}{A_{\mathrm{eff}}}\right)[(0.5283\tilde{p}^o)^{1/7} - 1] \qquad \tilde{p}^o \geq 1.893 \tag{31}$$

The previous analysis represented theoretical model of the choked (supercritical) outflow. On the other hand, for the subcritical (subsonic) outflow, we have

$$\frac{\mathrm{d}p_c}{\mathrm{d}t} = \kappa RT_c(t)\left(\frac{\dot{m}_i}{V_c}\right) - \kappa RT_c(t)\left(\frac{A_{\mathrm{eff}}}{V_c}\right)\sqrt{\frac{2\kappa}{\kappa-1}\rho_c p_c[(\frac{p_a}{p_c})^{\frac{2}{\kappa}} - (\frac{p_a}{p_c})^{\frac{\kappa+1}{\kappa}}]} \tag{32}$$

Together with the chamber's isentropic temperature change relationships, this yields a complete mathematical model of subcritical decompression. After tedious reductions and rearrangements with the assumption of zero recompression, one obtains

$$\frac{\mathrm{d}\tilde{p}}{\mathrm{d}t} = -\left(\frac{A_{\mathrm{eff}}}{V_c}\right)\cdot\kappa\cdot\left(\frac{2\cdot\kappa}{\kappa-1}\right)^{1/2}\sqrt{R\cdot T_c^o}\cdot\tilde{p}^{o(\frac{1-\kappa}{2\kappa})}\cdot\tilde{p}^{\frac{3(\kappa-1)}{2\kappa}} \cdot(1-\tilde{p}^{\frac{1-\kappa}{\kappa}})^{1/2} \tag{33}$$

Separating the variables and integrating,

$$\int_1^{\tilde{p}}\frac{\mathrm{d}\tilde{p}}{\tilde{p}^{\frac{3(\kappa-1)}{2\kappa}}[1-\tilde{p}^{\frac{1-\kappa}{\kappa}}]^{1/2}} = -\left(\frac{A_{\mathrm{eff}}}{V_c}\right)\kappa\left(\frac{2\kappa}{\kappa-1}\right)^{1/2}\sqrt{RT_c^o}\tilde{p}^{o(\frac{1-\kappa}{2\kappa})}\cdot\int_0^{\tau}\mathrm{d}t \tag{34}$$

For air as a working fluid, the integral on the left-hand side represents isentropic PR function and can be obtained in closed-form via elementary functions:

$$\Phi_s(\tilde{p}) = \int_1^{\tilde{p}}\frac{\mathrm{d}\tilde{p}}{\tilde{p}^{\frac{3}{7}}[1-\tilde{p}^{\frac{-2}{7}}]^{1/2}} = \int_1^{\tilde{p}}\frac{\mathrm{d}\tilde{p}}{\tilde{p}^{\frac{2}{7}}[\tilde{p}^{\frac{2}{7}}-1]^{1/2}} = \frac{7}{4}\tilde{p}^{\frac{1}{7}}(\sqrt{\tilde{p}^{\frac{2}{7}}-1})\left(\tilde{p}^{\frac{2}{7}}+\frac{3}{2}\right) + \frac{21}{8}\ell_n[\tilde{p}^{\frac{1}{7}} + \sqrt{\tilde{p}^{\frac{2}{7}}-1}] \tag{35}$$

In particular, the integral between limits of subcritical outflow (1.893 to 1) yields a value of about 3.453. Using chamber air at 296 K, the total time elapsed during subcritical isentropic decompression is

$$\tau = 3.5\cdot 10^{-3}\left(\frac{V_c}{A_{\mathrm{eff}}}\right) \qquad \tilde{p}^o = 1.893$$
$$\Phi_s(1.893) = 3.452856638 \tag{36}$$

Interestingly, isothermal and isentropic PR functions do not differ much, with maximum difference being less than 3.4% at the very end of the interval, where PR = 1.893. Mavriplis [33] used the average value of these two functions in his calculations. By comparing Eqs. (21) and (36), we conclude that isentropic expansion is about 25% shorter than isothermal. In the case when decompression starts in the subcritical range (entirely only subsonic flow), and with the same air properties as above, the DT becomes

$$\tau = 9.26\cdot 10^{-4}\cdot\Phi_s(\tilde{p}^o)\cdot\tilde{p}^{o1/7}\left(\frac{V_c}{A_{\mathrm{eff}}}\right)$$
$$1 \leq \tilde{p}^o < 1.893 \qquad \Phi_s(1) = 0 \tag{37}$$

The total (super- and subcritical) DT for chamber air's isentropic expansion [Eqs. (31) and (36)] is thus

$$\tau \approx \left(\frac{V_c}{A_{\mathrm{eff}}}\right)\cdot[0.0228(\tilde{p}^o)^{1/7} - 0.0215] \qquad \tilde{p}^o \geq 1.893 \tag{38}$$

In the case of isentropic expansion, the time required for the cabin pressure to halve (DHT), provided the outflow remains choked, is

$$\Theta_{1/2} = \frac{0.0449}{(\frac{A_{\mathrm{eff}}}{V_c})\cdot\sqrt{T_c^0}} \qquad p_c = \frac{p_c^0}{2} \tag{39}$$

The DHT value cannot be simply doubled to arrive at the actual total DT, since outflow will necessarily slow down as the conditions in the throat of an opening transition to subcritical. For the initial chamber temperature of 296 K, the isentropic DHT without repressurization becomes particularly simple:

$$\Theta_{1/2} = 0.0026\cdot\left(\frac{V_c}{A_{\mathrm{eff}}}\right) \qquad \tilde{p}^o \geq 3.786 \tag{40}$$

The chamber temperature at this DHT is a fixed ratio of the initial cabin temperature and for 296 K, one can write with sufficient accuracy,

$$T_{c,1/2} = T_c^0\cdot\left\{\left[\frac{p_c(t)}{p_c^0}\right]^{\frac{\kappa-1}{2\kappa}}\right\}^2 = \frac{T_c^0}{[1+2.32\cdot(\frac{A_{\mathrm{eff}}}{V_c})\cdot\sqrt{T_c^0}\cdot\Theta_{1/2}]^2} \approx 0.82\cdot T_c^0 \tag{41}$$

This temperature and pressure half-time parameters provide simple, yet reliable, characterization of the rapid-decompression process and no separate diagram, such as in the H-C model [31], or other inputs or variables are required.

D. Model of the Cockpit Security Doors Hinged Panel Dynamics

A mathematical model of cabin-to-cockpit flow through the hinged (swinging) panels in the intrusion-proof sealed cockpit security door is presented. We assume two stainless-steel hinged panels with dimensions of 30 × 30 cm and 1 cm thickness. No particular commercial model of the cockpit security door is modeled. The analysis presented here can also be applied to other venting passages between different pressurized airplane chambers (dado panels).

The hinged panels may be protected by screens on the cabin side. The panels are prestressed with a torsion spring at 300 Nm to withstand the force of 2 kN (450 lb) in the center of the panel. When the threshold pressure differential of about 22.2 kPa (3.22 psi) is reached between the cabin and the cockpit, the panels start swinging to open. The outflow area will be the function of the pressure differential and the panel opening angle θ.

The FAA regulation Title 14 CFR Part Sec. 25.795 [20] for large transport-category airplanes requires the cockpit security door to withstand the impact of 300 J (Nm) at its weakest point. That would

correspond to a 150 kg (330 lb) person running into the security door at 2 m/s (6.6 ft/s) or an almost 67 kg (148 lb) person hitting the door at 3 m/s (9.9 ft/s).

The schematic of the cockpit security door and the hinged panels is shown in Fig. 4. The conservation of the angular momentum for the individual hinged panel yields

$$I \cdot \frac{\mathrm{d}^2\theta}{\mathrm{d}t^2} = \sum_i M \tag{42}$$

The moments (torques) acting on the single hinged panel are

$$\sum_i M = (A_p \cdot \cos\theta) \cdot \Delta p(t) \cdot \frac{b}{2} \cdot \cos\theta - \tau_0 - k \cdot \theta - W_p \cdot \sin\theta \cdot \frac{b}{2} - \xi \frac{\mathrm{d}\theta}{\mathrm{d}t} \tag{43}$$

where the detent torque can be calculated from the pressure (force) required to starting opening the panels:

$$\tau_0 = \Delta p^* \cdot A_p \cdot \frac{b}{2} = \Delta p^* \cdot \frac{ab^2}{2} = F^* \cdot \frac{b}{2} \tag{44}$$

The momentum on the panel is proportional to the pressure differential. The resultant force acts in the center of pressure. The moment of inertia of a rectangular panel ($a = 0.3$ m and $b = 0.3$ m) and thickness ($\delta = 0.01$ m) is

$$I = \frac{W_p \cdot b^2}{3 \cdot g} = \frac{m_p \cdot b^2}{3}$$

The mass of the stainless-steel hinged panel ($\rho_p = 7450$ kg/m^3) is $m_p = a \cdot b \cdot \delta \cdot \rho_p = A_p \cdot \delta \cdot \rho_p$, where $A_p = a \cdot b$ is the surface area of the door. The differential equation for the hinge angle is, accordingly,

$$I \cdot \frac{\mathrm{d}^2\theta}{\mathrm{d}t^2} = \Delta p(t) \cdot A_p \cdot \frac{b}{2} \cdot \cos^2\theta - \tau_0 - k \cdot \theta - m_p \cdot g \cdot \sin\theta \cdot \frac{b}{2} - \xi \frac{\mathrm{d}\theta}{\mathrm{d}t}$$

$$IC\text{: } t = 0 \qquad \theta = 0 \qquad \dot{\theta} = 0 \qquad \theta \geq 0 \quad \forall\ t = [0, \infty)$$

$$\Delta p(t) = p_{cb}(t) - p_{cc}(t) \tag{45}$$

The open area for communication between the cabin and the cockpit for two panels will be the function of the hinge angle:

$$A_{\text{open}}(\theta) = 2 \cdot a \cdot b \cdot \sin\theta + a^2 \cdot \sin\theta \cdot \cos\theta \tag{46}$$

The discharge coefficient will also be a function of the hinge angle. We propose the following relationship, which also includes the resistance of screens in front of the panels:

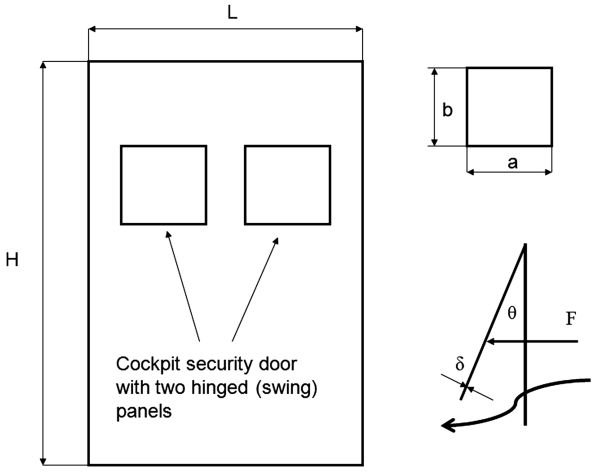

Fig. 4 Schematic of cockpit security door with two hinged swinging panels.

$$c_D(\theta) = c_{D0} + 0.5 \cdot \sin\theta$$

where $c_{D0} = 0.3$.

The panels can only open in the direction of the cockpit. The panels cannot rotate toward the cabin past the stops in the panel frame. This is also to prevent cockpit depressurization if the cabin depressurizes first. Cockpit pressure can vent through dado panels to prevent excessive force on the cockpit door. The spring that resists the opening of the hinged panels is assumed to be linear within its working range. However, it would present no problem to include hard- or soft-spring effects. The prestressed static resistance must be overcome first before the hinged panels start to open. The hinged panels are flushed closed due to the prestressed torsion spring, $\tau(\theta) = \tau_0 + k \cdot \theta$, with $\tau_0 = 300$ Nm, and $k = 175$ Nm/rad.

The implication of this is that the pressure difference needs to reach about 22.2 kPa (3.22 psi) before the panels start opening. The temporal force on the door can be calculated at any time as

$$F_d(t) = \Delta p(t) \cdot (A_D - 2 \cdot a \cdot b \cdot \sin\theta) \qquad A_D = H \cdot L \tag{47}$$

This force can reach extreme values and stay high for extended periods, which could possibly dislocate the door from the frame and blow it into the cockpit with the catastrophic consequences. The strongly nonlinear second-order ODE for panel hinge angle is now

$$I \cdot \frac{\mathrm{d}^2\theta}{\mathrm{d}t^2} + \xi \frac{\mathrm{d}\theta}{\mathrm{d}t} + k \cdot \theta + m_p \cdot g \cdot \sin\theta \cdot \frac{b}{2} - \Delta p(t) \cdot A_p \cdot \frac{b}{2} \cdot \cos^2\theta = -\tau_0$$

$$t = 0 \qquad \theta = 0 \qquad \frac{\mathrm{d}\theta}{\mathrm{d}t} = 0 \qquad \theta \geq 0 \quad \forall\ t = [0, \infty) \tag{48}$$

The pressure differential provides a normal force that is dependent on the hinge angle θ. Both hinged panels will start opening after the pressure difference of 22.2 kPa has been reached between the cabin and the cockpit. The panels may swing past 90°, which would be caused by rotation inertia. Oscillations in hinged panel rotations are certainly to be expected, and the amount of damping in the hinge mechanism controls the decay of oscillation amplitudes. Although oscillating, the panels will be closing on average, due to prestressed spring torque, weight, and the decreasing pressure differential between the cabin and the cockpit. Once the pressure differential drops below 22.2 kPa (3.22 psi), the panels will stay closed. Thus, the cabin will end up at a somewhat higher pressure (lower CA) than the cockpit, which would provide additional benefit. In reality, passive and active vents would increase cabin pressure altitude further, albeit with some delay. The outflow through the two door panels will be choked or subcritical, depending on the pressure ratio between the uniform cabin and cockpit pressures.

III. Methods and Materials

A. Aircraft Configurations

We used two different airplane types in decompression simulations. The first is The Boeing Company's commercial twin-engine heavy jet B767-300ER (extended range) and is currently still the most popular and most common airplane on long-range routes. Boeing 767-300ER has a net cockpit volume of 8 m^3 (282 ft^3) and the net available cabin and cargo (aft and forward) air volume of about 980 m^3 (34, 582 ft^3). The maximum pressure differential for the pressure vessel is 8.6 psi (59.31 kPa). The second aircraft for which decompression events were simulated is a new Raytheon business jet: Hawker 4000. The Hawker's cockpit volume is 150 ft^3 (4.25 m^3) and the cabin has a net volume of 762 ft^3 (21.58 m^3). The Hawker 4000 has maximum structural pressure differential of 9.8 psi (67.58 kPa) and can maintain SL cabin altitude up to 25,240 ft (7,695 m). The limitation of maximum structural pressure differential was strictly observed in simulations for each airplane model.

The uniform atmospheric pressure at the effective FL 390 is 19.68 kPa (2.85 psi), and the cabin pressure of 78.959 kPa (11.45 psi or about 6500 ft CA) was used for B767. This corresponds to the

B767-300ER's maximum structural pressure differential. The Hawker 4000 pressure vessel can sustain larger maximum pressure differential, and the cabin pressure used in simulations was 12.65 psi (87.23 kPa or about 4000 ft CA), resulting in lower CA than B767 with the fully closed outflow valve(s). The uniform cabin and cockpit temperature was 23°C (296 K) for both airplane models. The effect of the local atmospheric pressure and air velocity distribution has been replaced by the equivalent ISA altitude and local static environmental pressure. The ISA model was used to describe the environmental changes with altitude [44].

B. Numerical Simulation

The in-house-developed simulation program based on the MATLAB platform was used. Numerical integration of the set of coupled nonlinear first-order ODEs was performed using the MATLAB ODE solver ode23s. This solver has an adaptive step-size feature obtained through solving the ODE using the second- and the third-order Runge–Kutta methods. This methodology is applicable to stiff systems, in which multiple time constants coexist [40–43,45–47]. The initial time step used was 20–25 ms for slower decompressions, down to 0.1–10 ms for faster decompressions. The iterations were monitored to stop the integration process when the relative difference between temporal neighboring points was small. The friction coefficient in the panel door was set to 0.1 and the discharge coefficient was set to 0.8 for the window frames and all other geometries. Three rupture sizes were simulated: 1, 0.1, and 0.01 m^2 (e.g., 10×10 cm square opening). For Hawker 4000, we did not use the cockpit rupture sizes of 1 m^2, as that would probably result in a catastrophic structural failure, considering the airplane overall size. Each panel door weighs about 6.7 kg, and we assumed that the same cockpit door was installed in both airplane types.

C. Decompression Model Verifications

Let us compare DTs derived here with those derived by Haber and Clamann [31] and Fliegner (as reported in [3]). Fliegner's equation for DT with volume in cubic meters and surface area in meters squared is

$$\tau = 0.005 \cdot \left(\frac{V_c}{A_{\text{eff}}}\right) \cdot \sqrt{\tilde{p}^o - 1} \tag{49}$$

H-C's total DT equation yields

$$\tau = \left(\frac{V_c}{A_{\text{eff}} \cdot a}\right) \cdot P_1\left(\frac{p_c^o - p_a}{p_c^o}\right) = \left(\frac{V_c}{A_{\text{eff}}}\right) \cdot \frac{1}{a} \cdot P_1\left(1 - \frac{1}{\tilde{p}^o}\right) = \tau_c \cdot P_1\left(1 - \frac{1}{\tilde{p}^o}\right) \tag{50}$$

where P_1 is a complex function depending on the relative PR and obtained from the H-C diagram [31]. It needs to be said here that the longer the decompression, the more polytropic the expansion process becomes, as the heat transfer and other irreversible processes cannot be neglected.

The comparison between our isentropic and isothermal theoretical models and those of H-C and Fliegner for various volume-to-area V/A ratios is shown in Fig. 5. The Fliegner model [Eq. (49)] actually yields DTs longer than for isothermal decompression, which is physically impossible in spontaneous expansion unless extra heat is added to the system. Fliegner's model could be used practically only as an approximation of the isothermal decompression. As expected, the H-C data, which has become a standard in decompression analysis, is located between our isothermal and isentropic results. This is not surprising, as the H-C model is based on some ensemble-averaged typical decompression. H-C's polytropic expansion is slightly closer to isothermal than to isentropic decompression. The H-C model is slightly less accurate for very rapid aircraft decompressions.

An important aspect of our mathematical model and computer simulations is verification and comparison with experimental data and/or other models. Incredibly, not much has been published on the

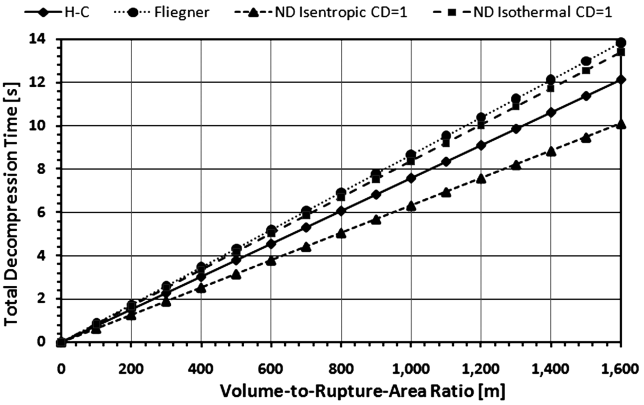

Fig. 5 Comparison of different theoretical models of chamber decompression for the initial PR of 4.0 (80/20 kPa) and variable V/A ratio. H-C's PR is $(80 - 20)/80 = 0.75$.

phenomenon of aircraft decompression, and no direct experiments of actual aircraft decompression exist to the best of our knowledge. However, some limited references exist on the decompression (and pressurization) of pressurized vessels, pipes, etc. In several research projects, Daidzic [40–43] obtained many experimental results and created mathematical model with computer simulation code of pressurization dynamics in preignition flow transients in a liquid oxygen (LOX) dome of Messerschmitt-Bölkow-Blohmn's HM-7B third-stage rocket engine for rocket launcher Ariane IV. The isentropic model was able to predict pressure ramps of up to 2–3 MPa/s extremely well. This pressure ramps were used to simulate the starting cycle of turbopumps supplying LOX for ignition. Experiments and modeling of LOX injector elements also demonstrated the accuracy of the isentropic compression models.

Chan [48] presented numerical and experimental data on depressurization of pressurized vessels. We made several comparisons with Chan's experimental data. In Fig. 6, we compared Chan's data for constant $V/A = 1171.1$ m. The air in Chan's high-PR experiments was at RH of 80% and about 20 K warmer than air in our simulations. Obviously, condensation and warmer air will slow down the depressurization process, explaining the difference of several hundred milliseconds or 6.25% at the higher PR with $C_D = 1.0$ in our model. However, when we used $C_D = 0.9$, the fit was almost perfect. It appears that by adjusting the C_D in our isentropic model, we can simulate all additional effects, such as diabatic conditions, polytropic change, etc.

In Fig. 7, we show the time history of the pressure change as a function of time using our isentropic model with $C_D = 0.9$ and Chan's [48] experimental pressure measurements. The fit is almost perfect. Because of latent heat of condensation of the very humid air in Chan's experiment, the temperature drop shows a large discrepancy of 20–30 K compared with our isentropic simulations.

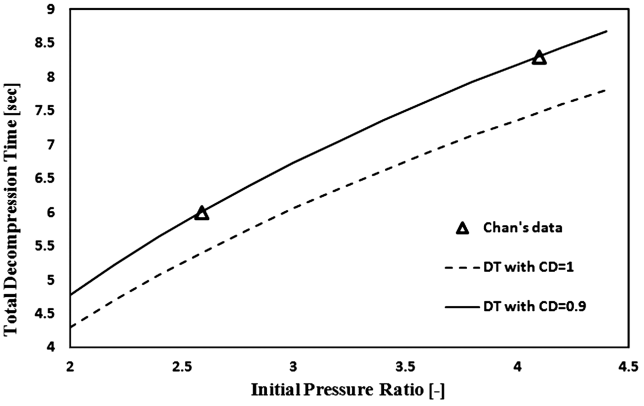

Fig. 6 Comparison of isentropic model DT with Chan's [48] experiment for two distinct PRs of 2.59 and 4.08, RH = 80% air, and $V/A = 1171$.

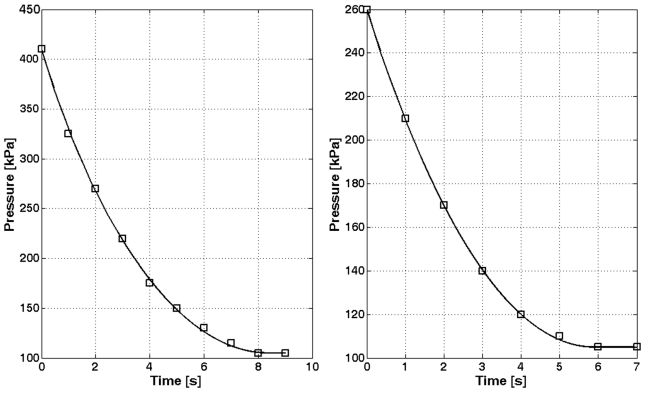

Fig. 7 Comparison of our isentropic model pressure history with Chan's [48] experiments for two distinct PRs of 4.08 and 2.59.

Chan stated in his work that he had problems with temperature measurements. Fortunately, an airplane's air is much drier, and that works to our benefit in using an isentropic model without condensation.

The comparison of Veldman's [49] experimental DTs, H-C's theory, and our isentropic model is shown in Fig. 8. The initial PR is 1.517 and therefore entirely in subcritical outflow regime. Veldman's experimental results for an air storage tank and long PVC pressurized pipe (simulating aircraft fuselage) was used for experimental verification. One can observe a small difference between H-C and our isentropic model with $C_D = 1$ for small V/A ratios or short DTs. For larger DT and V/A ratios, our isentropic model with $C_D = 0.85$ gives a better fit than H-C's. However, Veldman [49] did not provide any information on RH of air, heat transfer, or discharge coefficient, which might have affected expansion rates in his experiments. Nevertheless, our simulation results are within standard deviation of Veldman's experimental data, giving us additional confidence in our isentropic model being quite reliable at mimicking rapid aircraft decompressions.

IV. Simulation and Discussion of Results

A. Cabin Decompression

In Fig. 9, the B767-300ER's cabin pressure and temperature history is given during decompression caused by the cabin rupture of 0.1 m^2. The cockpit will not depressurize. The supercritical flow from about 79 kPa down to about 37 kPa took about 34 s, which is consistent with the theoretically obtained results. The subcritical decompression continues for about another 44 s, until the outside atmospheric pressure is practically reached. The transition from critical to subcritical decompression is smooth. Simultaneously, the isentropic expansion will result in rapid cooling of the cabin air. After about 60 s, the cabin temperature dropped from a comfortable 23°C to almost −62°C. In reality, the water vapor in the cabin air would condense and freeze or create mist of ice crystals by deposition/sublimation, but we neglected the effect of the released latent heat of condensation and freezing, which resulted in the absolutely minimum air temperature possible. Ultimately, the heat transfer will work to equalize the temperature inside and outside of the airplane once decompression is completed, resulting in a temperature of around −57°C if the airplane maintains altitude without emergency descent. From Fig. 9, one can also observe that the total DT is about 78 s for an effective cross-sectional area of 0.08 m^2 and $V/A_{\text{eff}} = 12,250$ m. The pressure rate curve flattens out as the cabin pressure asymptotically approaches the environmental pressure. A lot of time elapses for the pressure to drop a practically insignificant amount. Therefore, the pressure DHT might be a more reasonable parameter to use. Our isentropic model predicts DHT of 31.9 s. After that period, the cabin pressure dropped to about 39.5 kPa, which is still in the critical-flow regime. The transition to subcritical outflow occurs at 37.25 kPa.

In Fig. 10, the B767-300ER's cabin pressure and temperature histories are given for a 1 m^2 cabin rupture, which is 10 times larger area than in the previous example. The same discharge coefficient $C_D = 0.8$ was used, resulting in $V/A_{\text{eff}} = 1225$ m. The decompression to environmental pressure of about 20 kPa occurred in 7.8 s, which is also 10 times faster than in the previous example with a larger V/A ratio. The cabin temperature reached the same −75°C, but now in much shorter period. Obviously, such conditions would be harsh for occupants and can be reached before the crew even initiates emergency descent.

Let us now examine the decompression dynamics of a typical midsize corporate jet: Hawker 4000. In Fig. 11, the pressure and temperature histories for the rupture area of 0.1 m^2 (e.g., circular hole of 18 cm in diameter) and $C_D = 0.8$ are shown. As expected, due to the small V/A_{eff} (270 m) ratio, the DT is very short. In less than 1.8 s, the initial pressure differential of 67.6 kPa was reduced to zero. The initial PR was 4.43. The temperature dropped to −80°C for the same time period. The DHT is 0.7 s, which is very close to the simulated value.

In Fig. 12, the pressure and temperature histories for Hawker 4000 and $V/A_{\text{eff}} = 27$ (the rupture area of 1 m^2 and $C_D = 0.8$) are shown. The cabin depressurization is of the explosive type, with possible severe physiological consequences for occupants. Such a large rupture in a relatively small airplane could possibly result in a complete loss of hull due to excessive aerodynamic loads. The DHT is 70 ms. Accordingly, and as expected, the corporate jets are more hazardous for occupants than the large-transport-category civilian airplanes with respect to rapid decompressions. In addition, many corporate jets have higher structural pressure differentials and fly at higher altitudes, which could make things even worse.

B. Cockpit Decompression

In Fig. 13, the effect of a B767's cockpit depressurization ($V/A_{\text{eff}} = 10$ m) on the cabin pressure, loads, and dynamics of the

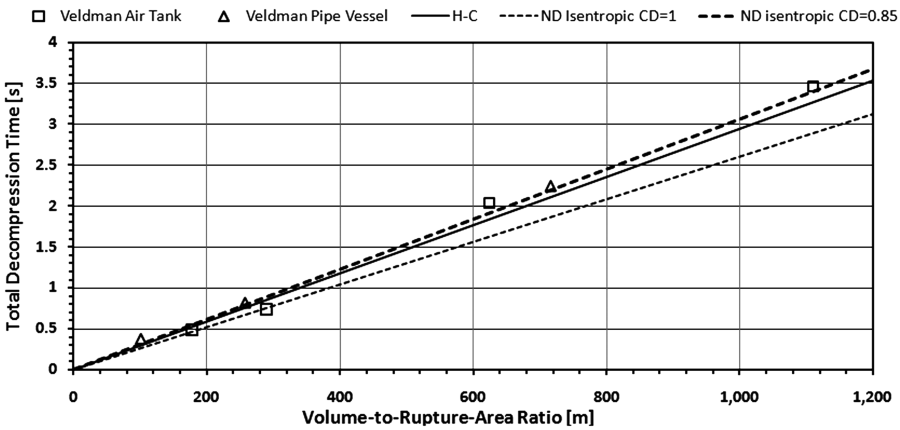

Fig. 8 Comparison of Veldman's [49] experimental results and theoretical H-C's and (ND) isentropic model DTs for the subcritical initial PR of 1.517 (151.7/100 kPa). H-C's PR is (151.7 − 100)/151.7 = 0.341.

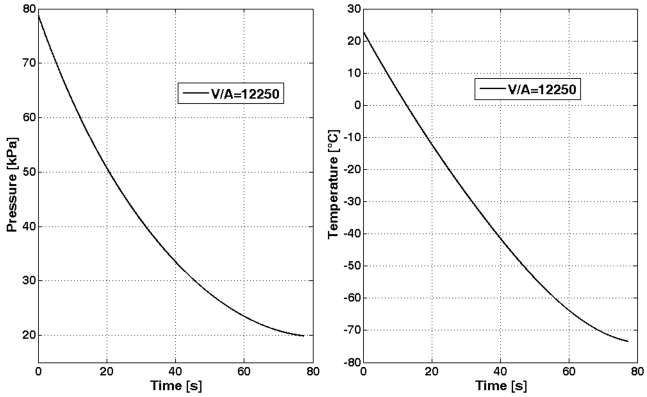

Fig. 9 Boeing 767-300ER cabin pressure and temperature history for closed cockpit door, cabin rupture of 0.1 m^2.

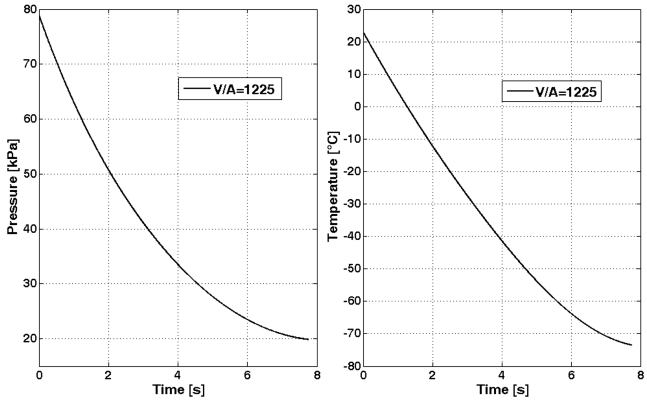

Fig. 10 Boeing 767-300ER cabin pressure and temperature history for closed cockpit door and cabin rupture of 1 m^2.

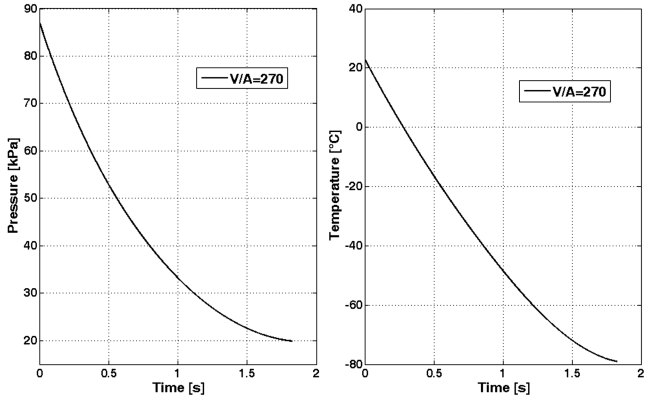

Fig. 11 Hawker 4000 cabin pressure and temperature history for closed cockpit door and cabin rupture of 0.1 m^2.

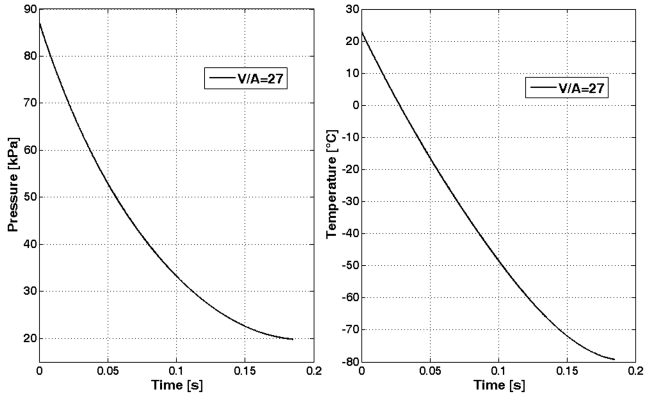

Fig. 12 Hawker 4000 cabin pressure and temperature history for closed cockpit door and cabin rupture of 1 m^2.

swinging panels is shown. In all cockpit depressurization simulations, it was assumed that the complete, or a portion of the, side window broke up suddenly and instantaneously. The window rupture size is 1 m^2 with no RAM pressure recovery. Obviously, the cockpit depressurized rapidly and expansion was finished in 60 ms, accompanied by severe temperature drop. Clearly, this scenario is very hazardous for the flight crew. The pressure drop rate is 983.3 kPa/s or 142.6 psi/s. The cabin started depressurizing after the pressure differential between the cockpit and the cabin reached 22.2 kPa, which was almost instantaneously. However, due to the relatively small cross-sectional area of the pressure-equalizing hinged panels, the explosive cockpit decompression was not experienced with the same severity in the cabin. The temperature in the cabin dropped to only −25°C after 60 s, which is far warmer than a cockpit temperature of about −75°C. The hinged panels were swinging violently between 5 and 75°. Small oscillations were felt in the cabin air outflow and cabin pressure and temperature decay. The force on the security door exceeded 80 kN almost instantly and even after 5 s was still above 65 kN. The security door panels caused the cabin to depressurize about an order of magnitude slower. However, the powerful force on the door might have dislodged it from the frame and pushed into the cockpit.

In Fig. 14, the effect of a cockpit rupture of 0.1 m^2 with $C_D = 0.8$ in the B767 cockpit's side window is shown. The cockpit pressure and temperature drop rate is, as expected, slower. The force on the cockpit door reached almost 80 kN about 0.6 s after the sudden loss of cockpit pressure. The swinging hinged doors reached a maximum deflection angle of 60°. The frequency and the amplitude of panel oscillations were smaller in this case. The cabin decompression dynamics was hardly influenced by the smaller cockpit rupture. The reason for this is that the cabin air has to communicate through the cockpit security door panels that act as a flow filter. Once the critical PR is reached (and exceeded) between the cockpit and the cabin, the cockpit decompression dynamics does not affect the cabin depressurization rates by any means.

In Fig. 15, the decompression history for an even smaller cockpit rupture of only 0.01 m^2 ($V/A_{\text{eff}} = 1000$ m) is shown. Since the cockpit depressurization is comparatively slow, the effect of time delay and the buildup of 22.2 kPa pressure difference between the cockpit and the cabin are evident in their respective temporal histories. It took more than 1 s for the hinged panels to start moving. The maximum force on the security door reached just over 64 kN, but then 6 s after the onset of sudden cockpit decompression. The frequency and the amplitude of swinging panel oscillations are relatively low, with the maximum panel deflection angle of about 40°. Interestingly, just as in all other cases here, the cabin-to-cockpit outflow never transitions to subcritical (it is always choked), as the critical PR is never reached, due to the panels closing at 22.2 kPa pressure difference, resulting in about 42 kPa absolute final cabin pressure. The cockpit pressure relaxed to atmospheric in about 6.2 s, whereas the cabin pressure was still in the 70 kPa range, thus ensuring critical flow through the swinging panels for the entire period.

The decompression history for the Hawker 4000 with the cockpit rupture of 0.1 m^2, and $C_D = 0.8$ ($V/A_{\text{eff}} = 53$) is shown in Fig. 16. The time delay between a hinged panel's first movement and the cabin pressure and temperature decay is evident again. The force on the security door reached almost 65 kN about 0.33 s after the cockpit rupture suddenly occurred. The frequency of the panel oscillations is about 8 Hz and they oscillated between the maximum of 55° and the frame stops. The oscillations in the normal force, cabin pressure, and temperature are a result of the intermittent closing and opening of the hinged panels. Again, the final pressure difference of 22.2 kPa was established after less than 2 s and the critical/supercritical outflow persisted during the entire depressurization.

In Fig. 17, the decompression history for the Hawker 4000 corporate jet with the cockpit rupture of 0.01 m^2, and $C_D = 0.8$ ($V/A_{\text{eff}} = 531$) is shown. The time delay is evident yet again, due to the relatively slow cockpit decompression. The force on the door reached almost 40 kN about 1 s after cockpit rupture suddenly occurred. The frequency of the panel oscillation is about 7 Hz and it oscillated between a maximum of 26° and the frame stops. That

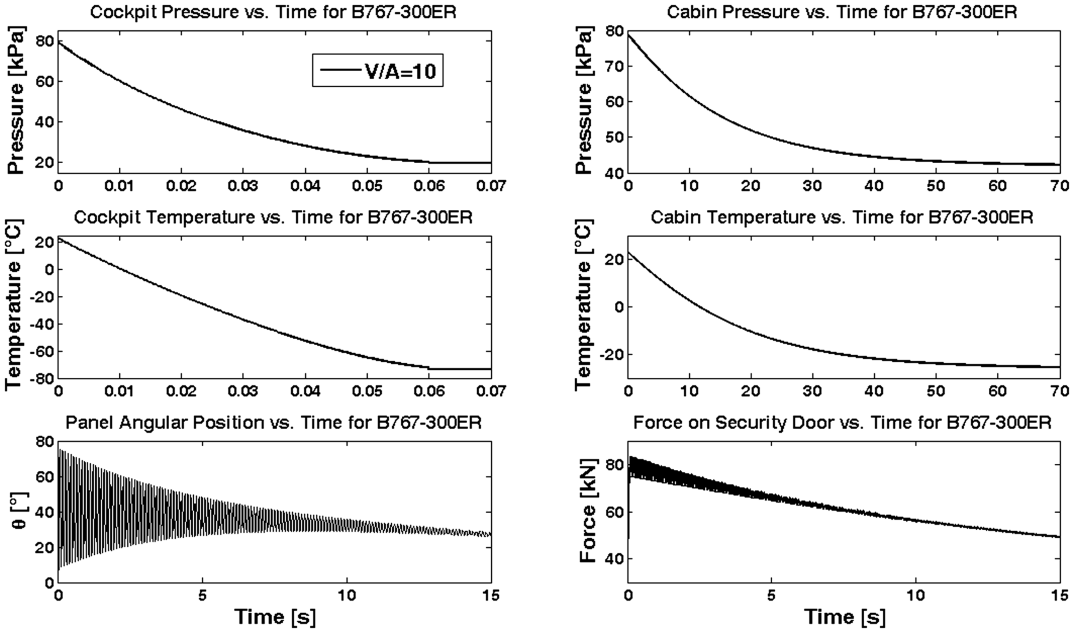

Fig. 13 Boeing 767-300ER cabin and cockpit history for closed cockpit door and rupture size of 1 m^2 in the cockpit side window with discharge coefficient of 0.8.

resulted in the cabin outflow occasionally completely stopping, due to the closure of the hinged panels. At these moments, the pressure force reached maximum. Interestingly, both the cabin and the cockpit depressurized in 4 s. This can be explained by the fact that the cockpit rupture was relatively small and of the size that panels could follow easily. The choked outflow persisted throughout the entire decompression, resulting in the equilibrium pressure difference of 22.2 kPa.

As a general conclusion, we observe that larger effective ruptures cause larger peak forces on the reinforced cockpit door, but the duration of the maximum normal force is shorter than in the case of slower cockpit decompressions, in which the peak force is lower but the duration is longer. The cockpit safety door ensures less severe decompressions in the cabin, performing as a dampening filter between them.

Let us now discuss the uncertainty of the DTs due to the uncertainty in the discharge coefficient or the effective rupture cross-sectional area. As the effective rupture size is the product of the discharge coefficient and the geometric rupture area, a law of reciprocity kicks in; infinitely many combinations will yield the same effective rupture area. Therefore, in the uncertainty analysis, it is sufficient to talk about the uncertainty of the effective surface area. The relative uncertainty in respect to effective outflow area only of the total isentropic DT [Eq. (38)] is

$$\frac{\Delta\tau}{\tau} = -\frac{\Delta A_{\text{eff}}}{A_{\text{eff}}} = -\frac{\Delta C_D}{C_D} \tag{51}$$

Accordingly, decreasing or increasing the coefficient of discharge by 10% only will result in an equivalent change in the decompression time, but with reverse sign. The same conclusion would be drawn for the uncertainty in the geometric rupture size. The combined uncertainty due to discharge coefficient and geometric rupture size can be easily estimated as well. Therefore, one may conclude that the total DT is moderately sensitive to the uncertainty in the effective rupture size.

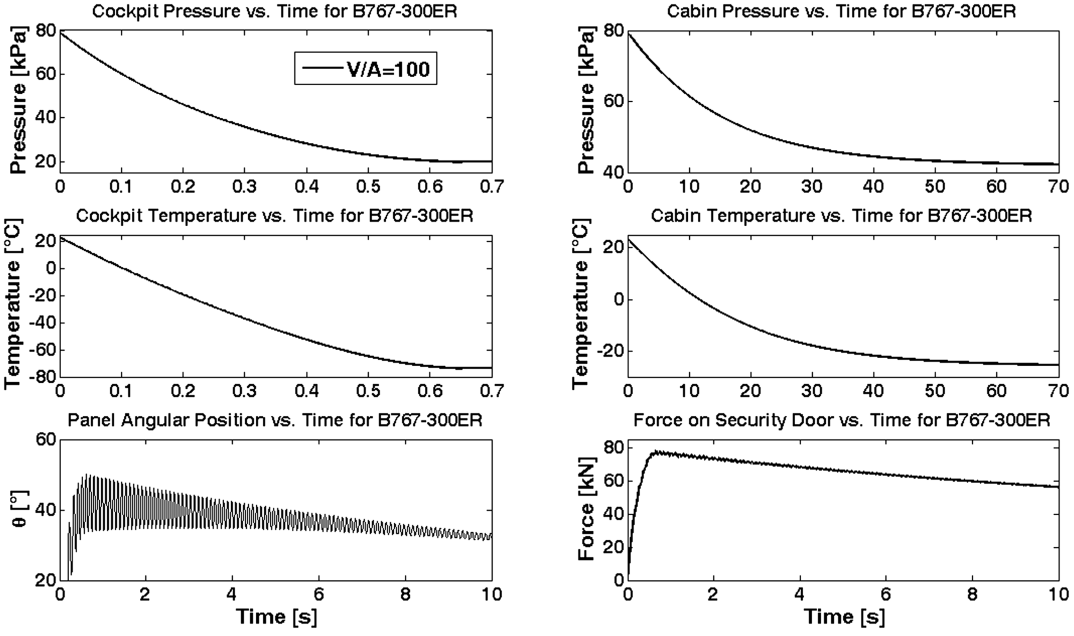

Fig. 14 Boeing 767-300ER cabin and cockpit history for closed cockpit door and rupture size of 0.1 m^2 in the cockpit side window.

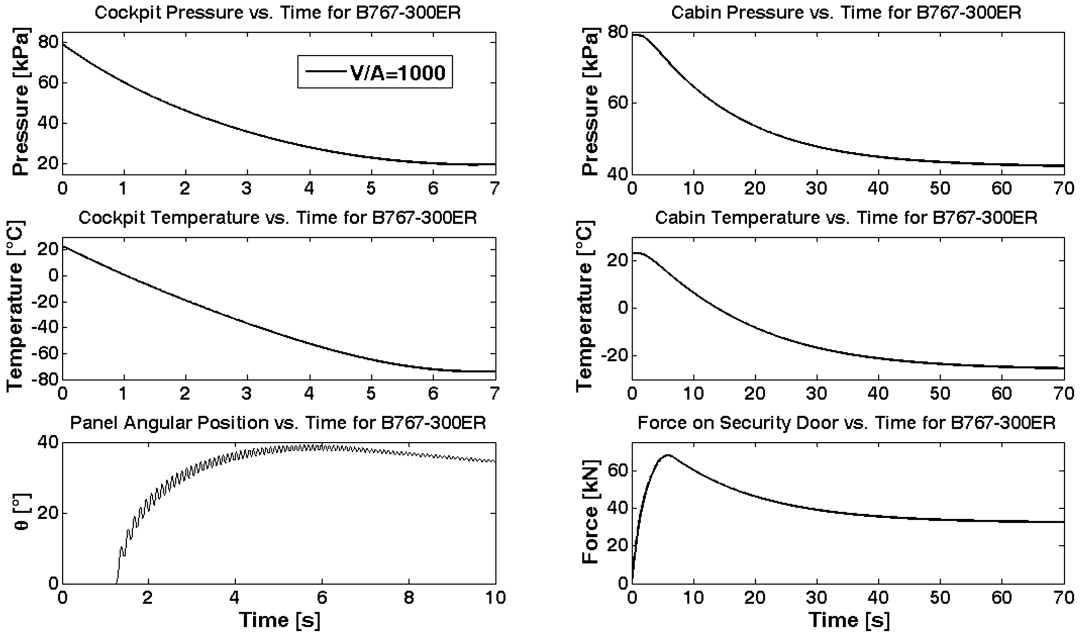

Fig. 15 Boeing 767-300ER cabin and cockpit history for closed cockpit door and rupture size of 0.01 m^2 in the cockpit side window.

The H-C theory is based on the ensemble-average of many decompression experiments. Some decompressions were faster than the others. The H-C expression for the total DT is based on the polytropic coefficient of expansion ($n = 1.16$), which was obtained as a minimum least-squares fit of 75 experiments [31]. As such, it averages across different decompression rates and is not particularly representative of rapid decompression on the time scales of less than 5 s. It is clear that the polytropic coefficient of expansion will change from 1.4 (isentropic) for rapid decompressions to 1.0 (isothermal) for slow decompressions. Therefore, our analytical expression for total isentropic DT is more accurate for short times than the H-C theory. In addition, our expression is far easier to calculate than H-C's and does not require any additional diagrams. We also think that the pressure DHT derived here offers the most representative and the simplest estimate of the depressurization dynamics. In any case, isentropic decompression represents the most severe loss of pressure occurrence and must be taken into account when designing ECSs.

We did not see any particular value in using higher-order spatially distributed computational codes at this point. The internal details and the flow resistances could vary significantly from airplane to airplane model as well as with respect to different loading and variable passenger seating in the same airplane model. The particular emphasis of this work was to investigate the coupling between the pressurized airplane chambers and the dynamic response of the security door's hinged panels. The basic motivation and the main purpose of this study were to focus on aviation safety and to emphasize possible dangerous scenarios if the cockpit depressurizes first and the security door becomes dislodged.

The future improvements in our model will include 1-D spatial modeling of all pressurized compartments, including forward and aft cargo, avionics compartment, etc. All of these different pressurized compartments will be connected through vent holes, swinging, and blowout panels, which provide passive and active venting between different pressurized compartments. That will result in additional equations for various pressurized compartments as well as ODEs for each panel dynamics. The emergency descent incorporating airplane aerodynamics will be fully modeled. The phase change of the water vapor and heat exchange will also be

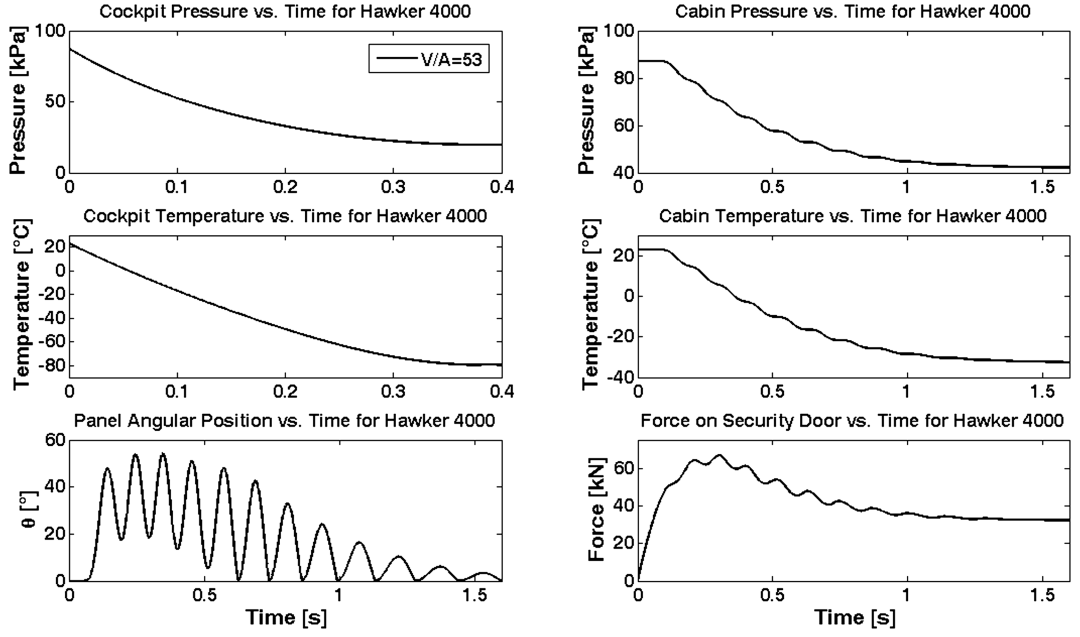

Fig. 16 Hawker 4000 cabin and cockpit history for closed cockpit door and rupture size of 0.1 m^2 in the cockpit side window.

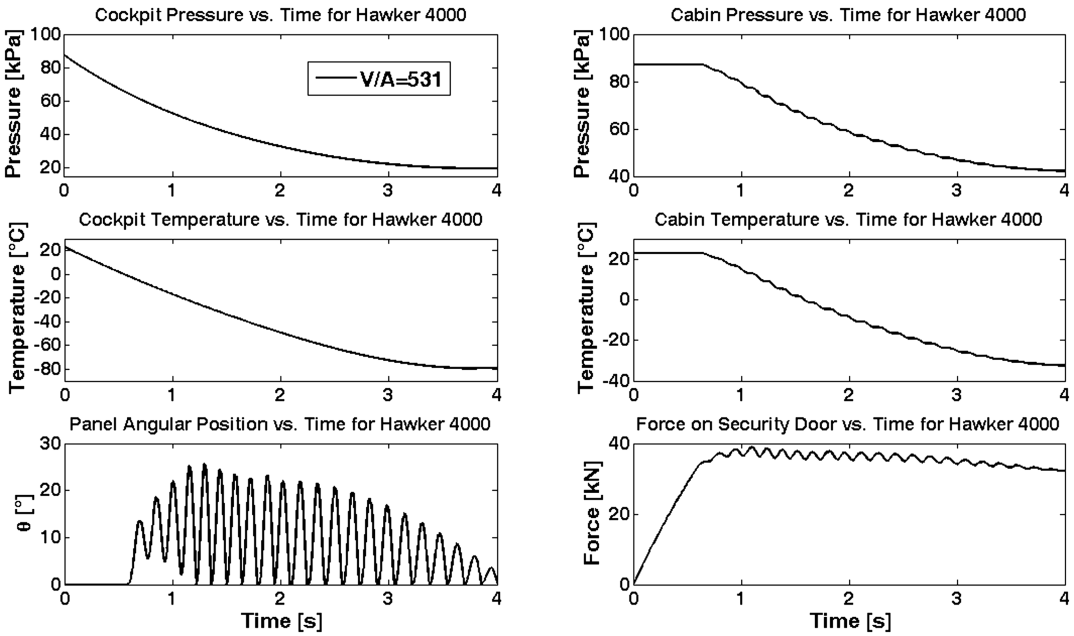

Fig. 17 Hawker 4000 cabin and cockpit history for closed cockpit door and rupture size of 0.01 m^2 in the cockpit side window.

considered. Carefully executed experiments using airplane scale models would do the most justice to the investigation of aircraft decompression in the absence of actual data.

V. Conclusions

We developed a zero-dimensional mathematical model of airplane cockpit and cabin decompression with an installed reinforced cockpit security door. Although relatively simple, the model and the accompanied simulation program performed sufficiently well. Analytical solutions for the critical and subcritical outflow were given in the case of isothermal and isentropic chamber decompression with the irreversible outflow. New analytical relationships were derived that provide quick estimate of the total decompression times for rapid decompressions as well as for very slow decompressions. A comparison with other theoretical decompression models and limited experimental data was conducted. The pressure half-time was defined, for which the temperature decay is always a fixed fraction of the initial chamber temperature, assuming isentropic expansion. ISA conditions were used to compute the atmospheric parameters. A nonlinear model of the swinging panels enabled the numerical experimentation with different cockpit decompression scenarios and its overall effects on the cabin pressure dynamics. This model can be extended to any case of venting, using swinging or blowout panels between various pressurized chambers/compartments. The force created on the security door due to pressure differential in some instances exceeded 80 kN instantaneously and reached steady value of 32 kN with panels fully closed. Faster cockpit decompression created higher peak normal forces, but of shorter duration. Slower cockpit decompressions produced lower peak forces that lasted longer. This is certainly valuable information to be considered when designing and installing security doors.

Acknowledgment

The first author would like to thank Chris Lykins, former undergraduate student in Minnesota State University's aviation program and now the first officer on the CRJ-200 regional jet for Mesaba Airlines, for his assistance in the early stage of this research.

References

[1] Ward, J. E., "The True Nature of the Boiling of Body Fluids in Space," *Journal of Aviation Medicine*, Vol. 27, 1956, pp. 429–439.

[2] Dunn, J. E., Bancroft, R. W., Haymaker, W., and Foft, J. W., "Experimental Animal Decompressions to Less Than 2 mm Hg Absolute: Pathologic Effects," *Aerospace Medicine*, Vol. 36, 1965, pp. 725–732.

[3] Bancroft, R. W., "Pressure Cabins and Rapid Decompression," *Aerospace Medicine*, 2nd ed., edited by H. W. Randel, Vol. 16, Williams & Wilkins, Baltimore, MD, 1971, pp. 337–363.

[4] Holmstrom, F. M. G., "Hypoxia," *Aerospace Medicine*, 2nd ed., edited by H. W. Randel, Vol. 5, Williams & Wilkins, Baltimore, MD, 1971, pp. 56–85.

[5] Sharp, G. R., and Ernsting, J., "Prevention of Hypoxia at Altitudes Below 40,000 Feet," *Aviation Medicine: Physiology and Human Factors*, edited by G. Dhenin, Tri-Med Books, London, 1978, Chap. 5, pp. 84–128.

[6] Simons, D. G., and Archibald, E. R., "Selection of Sealed Cabin Atmosphere," *Journal of Aviation Medicine*, Vol. 29, No. 5, 1958, pp. 350–357.

[7] Sharp, G. R., "Prevention of Hypoxia at Altitudes Above 40,000 Feet," *Aviation Medicine: Physiology and Human Factors*, edited by G. Dhenin, Tri-Med Books, London, 1978, Chap. 6, pp. 128–151.

[8] Sharp, G. R., "The Pressure Cabin," *Aviation Medicine: Physiology and Human Factors*, edited by G. Dhenin, Tri-Med Books, London, 1978, Chap. 7, pp. 151–176.

[9] Garner, R. P., "Concepts Providing for Physiological Protection After Cabin Decompression in the Altitude Range of 60,000 to 80,000 Feet Above Sea Level," U.S. Dept. of Transportation, Rept. DOT/FAA/AM-99/4, Feb. 1999.

[10] Hackworth, C., Peterson, L., Jack, D., Williams, C., and Hodges, B. E., "Examining Hypoxia: A Survey of Pilots' Experiences and Perspectives on Altitude Training," U.S. Dept. of Transportation, Rept. DOT/FAA/AM-03/10, May 2003.

[11] Hackworth, C., Peterson, L., Jack, D., and Williams, C., "Altitude Training Experiences and Perspectives: Survey of 67 Professional Pilots," *Aviation, Space, and Environmental Medicine*, Vol. 76, No. 4, 2005, pp. 392–394.

[12] Hawkins, G. S., and Southworth, R. B., "The Statistics of Meteors in the Earth's Atmosphere," *Smithsonian Contributions to Astrophysics*, Vol. 2, No. 11, 1958, pp. 349–363.

[13] Whipple, F., "On Meteoroids and Penetration," *Journal of Geophysical Research*, Vol. 68, No. 17, 1963, pp. 4929–4939.

[14] "Pressurized Cabins," *Code of Federal Regulations*, Title 14, CFR 25.841, Federal Aviation Administration, 1996.

[15] Macarthur, J., *Air Disaster*, Vol. 1, Aerospace Publications, Weston Creek, Australia, 1994, Chap. 1.

[16] Macarthur, J., *Air Disaster*, Vol. 2, Aerospace Publications, Weston Creek, Australia, 1996, Chaps. 10, 11.

[17] Bibel, G., *Beyond the Black Box: The Forensics of Airplane Crashes*, The Johns Hopkins Univ. Press, Baltimore, MD, 2008.

[18] National Transportation Safety Board Rept. CHI96IA157, Feb. 1998.

[19] National Transportation Safety Board Rept. CHI83IA054, Dec. 1983.

[20] "Security Considerations," *Code of Federal Regulations*, Title 14, CFR 25.795, Federal Aviation Administration, 2002.

[21] "Miscellaneous Equipment," *Code of Federal Regulations*, Title 14, CFR 121.313, Federal Aviation Administration, 2007.
[22] "Flightdeck Security," *Code of Federal Regulations*, Title 14, CFR 129.28, Federal Aviation Administration, 2003.
[23] Langley, M., "Decompression of Cabins," *Aircraft Engineering and Aerospace Technology*, Vol. 43, 1971, pp. 24–25.
[24] Wild, T. W., *Transport Category Aircraft Systems*, Jeppesen Sanderson, Englewood, CO, 1996.
[25] Pratt, J. D., "Rapid Decompression of Pressurized Aircraft Fuselages," *Journal of Failure Analysis and Prevention*, Vol. 6, No. 6, 2006, pp. 70–74.
doi:10.1361/154770206X156268
[26] "Notification and Reporting of Aircraft Accidents or Incidents and Overdue Aircraft, and Preservation of Aircraft Wreckage, Mail, Cargo, and Records," *Code of Federal Regulations*, Title 49, Part 830, Federal Aviation Administration, 1995.
[27] "Rapid Decompression in Air Transport Aircraft," Aviation Society of Aerospace Medicine, Balwyn, VIC, Australia, 2000.
[28] National Transportation Safety Board Rept. MIA01WA100, March 2001.
[29] National Transportation Safety Board Rept. NYC07LA121, May 2007.
[30] *Window Failure and Rapid Depressurization*, Transport Safety Board of Canada, Rept. A02A0046, April 2002.
[31] Haber, F., and Clamann, H. G., "Physics and Engineering of Rapid Decompression: A General Theory of Rapid Decompression," U.S. Air Force School of Aviation Medicine, Rept. 3, Randolph Field, TX, Aug. 1953.
[32] Demetriades, S. T., "On the Decompression of a Punctured Pressurized Cabin in Vacuum Flight," *Jet Propulsion*, Jan.–Feb. 1954, pp. 35–36.
[33] Mavriplis F., "Decompression of a Pressurized Cabin," *Canadian Aeronautics and Space Journal*, Dec. 1963, pp. 313–318.
[34] Jakovlenko, V. S., "Method of Calculating the Excess Pressure in Human Lungs Resulting from Cabin Decompression," *Kosmicheskaia Biologiia i Aviokosmicheskaia Meditsina*, Vol. 10, No. 5, 1976, pp. 62–68 (in Russian).
[35] Schroll, D. W., and Tibbals, T. F., "A Program for Analysis of Rapid Aircraft Cabin Decompression," *SAFE Association 37th Annual Symposium Proceedings*, Atlanta, Dec. 1999.
[36] Bréard, C., Lednicer, D., Lachendro, N., and Murvine, E., "A CFD Analysis of Sudden Cockpit Decompression," 42nd AIAA Aerospace Science Meeting and Exhibit, AIAA Paper 2004-0054, Reno, NV, Jan. 2004.
[37] Holman, J. P., *Thermodynamics*, 3rd ed., McGraw–Hill, Singapore, 1980.
[38] Hunt, E. H., and Space, D. R., "The Airplane Cabin Environment: Issues Pertaining to Flight Attendant Comfort," *International in-flight Service Management Organization Conference*, Montreal, Canada, Nov. 1994.
[39] Hunt, E. H., Reid, D. H., Space, D. R., and Tilton, F. E., "Commercial Airliner Environmental Control System: Engineering Aspects of Cabin Air Quality," *Aerospace Medical Association annual meeting*, Anaheim, CA, May 1995.
[40] Daidzic, N. E., "LOX Dome Investigation: Final Report," Lehrstuhl für Strömungsmechanik, Universität Erlangen-Nürnberg, Rept. LSTM 283/I/90, Erlangen, Germany, March 1990.
[41] Daidzic, N. E., "Experimental Investigation of Enlarged Injector Element LOX Post," Lehrstuhl für Strömungsmechanik, Universität Erlangen-Nürnberg, Rept. LSTM 311/I/90, Erlangen, Germany, March 1990.
[42] Daidzic, N. E., "Experimental Investigation of Transient Flow in HM-7B LOX Dome," Lehrstuhl für Strömungsmechanik, Universität Erlangen-Nürnberg, Rept. LSTM 310/I/90, Erlangen, Germany, March 1991.
[43] Daidzic, N. E., and Popp, M., "Transient Flow Behavior in a Rocket Engine Oxygen Dome," AIAA/ASME/SAE, 27th Joint Propulsion Conference, AIAA Paper 91-2280, Sacramento CA, June 1991.
[44] Anderson, J. D., Jr., *Introduction to Flight*, 6th ed., McGraw–Hill, Boston, 2008.
[45] Ferziger, J. H., *Numerical Methods for Engineering Applications*, Wiley, New York, 1981.
[46] Palm, W. J., III, *Introduction to MATLAB 7 for Engineers*, 2nd ed., McGraw–Hill, Boston, 2005.
[47] Chapra, S. C., and Canale, R. P., *Numerical Methods for Engineers*, 5th ed., McGraw–Hill, Boston, 2006.
[48] Chan, Y. S., "High-Pressure Reservoir Depressurization of Air with Condensation in Reservoir and Nozzle," M.S. Thesis, Univ. of Toronto, Toronto, Aug. 1990.
[49] Veldman, R. L., "Enhancing Commercial Aircraft Survivability via Active Venting," Ph.D. Thesis, Western Michigan Univ., Kalamazoo, MI, April 2001.